

# Diagnostics for Monte Carlo Algorithms for Models with Intractable normalising Functions

Bokgyeong Kang<sup>1</sup>, John Hughes<sup>2</sup>, and Murali Haran<sup>1\*</sup>

<sup>1</sup>Department of Statistics, Pennsylvania State University

<sup>2</sup>College of Health, Lehigh University

December 3, 2021

## Abstract

Models with intractable normalising functions have numerous applications ranging from network models to image analysis to spatial point processes. Because the normalising constants are functions of the parameters of interest, standard Markov chain Monte Carlo cannot be used for Bayesian inference for these models. A number of algorithms have been developed for such models. Some have the posterior distribution as the asymptotic distribution. Other “asymptotically inexact” algorithms do not possess this property. There is limited guidance for evaluating approximations based on these algorithms, and hence it is very hard to tune them. We propose two new diagnostics that address these problems for intractable normalising function models. Our first diagnostic, inspired by the second Bartlett identity, is, in principle, applicable in most any likelihood-based context where misspecification is of concern. We develop an approximate version that is applicable to intractable normalising function problems. Our second diagnostic is a Monte Carlo approximation to a kernel Stein discrepancy-based diagnostic introduced by Gorham and Mackey (2017). We provide theoretical justification for our methods and apply them to several algorithms in the context of challenging simulated and real data examples including an Ising model, an exponential random graph model, and a Markov point process.

*Keywords:* Bartlett identity, doubly intractable distributions, kernel Stein discrepancy, Markov chain Monte Carlo, sample quality measure, Ising model

---

\*Corresponding Author: muh10@psu.edu

# 1 Introduction

Models with intractable normalising functions arise in many contexts, notably the Ising (Lenz, 1920; Ising, 1925) and autologistic models (see Besag, 1974; Hughes et al., 2011, for a review) for binary data on a lattice, exponential random graph models (see Robins et al., 2007; Hunter and Handcock, 2006) for explaining relationships among actors in networks, and interaction point process models (see Strauss, 1975; Goldstein et al., 2015) for describing spatial patterns among points. Standard Markov chain Monte Carlo (MCMC) algorithms cannot be applied to these models. Suppose that we have data  $\mathbf{x} \in \mathcal{X}$  generated from a probability model with likelihood function  $L(\boldsymbol{\theta} \mid \mathbf{x}) = h(\mathbf{x} \mid \boldsymbol{\theta})/c(\boldsymbol{\theta})$ , where  $c(\boldsymbol{\theta})$  is a normalising function, and a prior density  $p(\boldsymbol{\theta})$ . The posterior density of  $\boldsymbol{\theta}$  is

$$\pi(\boldsymbol{\theta} \mid \mathbf{x}) \propto p(\boldsymbol{\theta}) \frac{h(\mathbf{x} \mid \boldsymbol{\theta})}{c(\boldsymbol{\theta})},$$

which brings about so-called doubly intractable posterior distributions. A major problem in constructing a standard MCMC algorithm for such models is that  $c(\boldsymbol{\theta})$  cannot be easily evaluated. The Metropolis–Hastings (MH) algorithm (Metropolis et al., 1953; Hastings, 1970) acceptance probability at each step requires evaluating the unknown ratio  $c(\boldsymbol{\theta})/c(\boldsymbol{\theta}')$ , where  $\boldsymbol{\theta}'$  denotes the proposed value.

A wide range of computational methods have been proposed for Bayesian inference for doubly intractable posterior distributions (see Park and Haran, 2018, for a review). There are asymptotically exact algorithms whose Markov chain has a stationary distribution equal to its target distribution (Møller et al., 2006; Murray et al., 2006; Atchadé et al.,

2013; Lyne et al., 2015; Liang et al., 2016). Throughout this manuscript we use “target distribution” to refer to the posterior distribution of interest. The algorithms of Møller et al. (2006) and Murray et al. (2006) require the ability to generate samples exactly from the probability model, which is available only for a small class of probability models having intractable normalising functions. The other asymptotically exact algorithms do not need exact sampling but are complicated to construct and have to be carefully tuned to provide reliable inference. These algorithms tend to be computationally intensive (Park and Haran, 2018). There are asymptotically inexact algorithms that may be much faster and can be applied to a wider class of problems (Liang, 2010; Alquier et al., 2016; Park and Haran, 2020). An asymptotically inexact algorithm either converges to an approximation of the target or is not known to converge to any distribution. The performance of these algorithms relies on the choice of various tuning parameters. It is also not always easy to judge the tradeoffs between using a faster asymptotically inexact algorithm and a potentially more computationally expensive but asymptotically exact algorithm. Hence, it is crucial to have diagnostics that provide guidance for users to carefully tune their algorithms to provide reliable results.

There is a large literature on convergence diagnostics for MCMC algorithms (see Cowles and Carlin, 1996; Flegal and Jones, 2011; Roy, 2020, for reviews). However, the literature on assessing the quality of approximations provided by asymptotically inexact algorithms is rather limited. Fan et al. (2006) proposed score function diagnostics that estimate some quantities whose values are known under the target distribution. Gorham and Mackey (2015) extended this idea and defined Stein discrepancies that measure the maximum devia-

tion between sample means and target expectations over a large class of test functions. Gorham and Mackey (2017) combined this approach with the theory of reproducing kernels and provided a closed-form kernel Stein discrepancy which has a theory of weak convergence analogous to that of Gorham and Mackey (2015). Lee et al. (2019) and Xing et al. (2019) provide some nice tools for assessing the coverage of approximate credible intervals. These are clever innovations but they are not available for asymptotically inexact algorithms for doubly intractable distributions. This motivates the development of diagnostic tools that assist scientists in tuning these algorithms. Following Gorham and Mackey (2017), we think of our diagnostics as measuring “sample quality.”

In this article we describe a new diagnostic method that uses the well known second Bartlett identity (cf. Bartlett, 1953a,b). Our method is, in principle, applicable in most any likelihood-based context where misspecification is of concern. We develop a Monte Carlo approximation to this new diagnostic that is applicable to intractable normalising function models. We also develop an approximate version of the kernel Stein discrepancy introduced by Gorham and Mackey (2017), making this available for doubly intractable distributions. This diagnostic asymptotically inherits the same convergence properties as that of Gorham and Mackey (2017) and thus can be used for diagnosing convergence of a sequence of sample points to the target distribution.

The remainder of this article is organized as follows. In Section 2 we briefly describe computational methods for models with intractable normalising functions. In Section 3 we discuss the need for diagnostics for tuning asymptotically inexact algorithms. In Section 4 we propose a new diagnostic for asymptotically exact and inexact methods, and we develop

an approximation for doubly intractable distributions. In Section 5 we briefly describe the kernel Stein discrepancy introduced by Gorham and Mackey (2017) and propose its Monte Carlo approximation for intractable normalising function models. We provide theoretical justification for our diagnostics. In Section 6 we describe the application of our diagnostic approaches to several algorithms in the context of three different challenging examples. Finally, in Section 7 we conclude with a brief summary and discussion.

## 2 Inference for models with intractable normalising functions

Several computational methods have been developed for Bayesian inference for models with intractable normalising functions. Park and Haran (2018) categorized these algorithms into two general, overlapping classes: (1) *auxiliary variable approaches*, which introduce an auxiliary variable and cancel out the normalising functions in the Metropolis–Hastings acceptance probability (Møller et al., 2006; Murray et al., 2006; Liang, 2010; Liang et al., 2016), and (2) *likelihood approximation approaches*, which directly approximate the normalising functions and plug the approximations into the Metropolis–Hastings acceptance probability (Atchadé et al., 2013; Lyne et al., 2015; Alquier et al., 2016; Park and Haran, 2020). An important characteristic of these algorithms is whether they are “asymptotically exact” or “asymptotically inexact.” Asymptotically exact algorithms generate samples whose asymptotic distribution is exactly equal to the target distribution. Asymptotically inexact algorithms generate samples that do not converge to the target distribution (or to any

distribution in some cases).

Asymptotically exact algorithms have attractive theoretical properties but can often be computationally burdensome or even infeasible for challenging models. For instance, Møller et al. (2006) and Murray et al. (2006) depend on perfect sampling (cf. Propp and Wilson, 1996), an algorithm that generates an auxiliary variable exactly from the target distribution using bounding Markov chains. Perfect samplers tend to be very computationally expensive and are available only for a small class of probability models. Atchadé et al. (2013) and Liang et al. (2016) propose asymptotically exact algorithms that do not need perfect sampling. These algorithms require storing simulated auxiliary data or its sufficient statistics with each iteration. The computational and memory costs are very expensive for models without low-dimensional sufficient statistics. Lyne et al. (2015) constructed an unbiased likelihood estimate for models with intractable normalising functions. To obtain a single estimate, their approach requires multiple Monte Carlo approximations to the normalising constant and thus can often be computationally prohibitive.

Several computationally efficient asymptotically inexact algorithms have also been proposed. For instance, the double Metropolis–Hastings (DMH) sampler, proposed by Liang (2010), replaces perfect sampling with a standard Metropolis–Hastings algorithm, an “inner sampler,” at each iteration. The DMH algorithm is easy to implement and is computationally efficient compared to the other algorithms discussed thus far. But the inner sampling becomes more computationally expensive with an increase in the dimension of the data. For large data problems, Park and Haran (2020) proposed a function emulation algorithm that approximates the likelihood normalising function (or full likelihood function) at several

parameter values and interpolates the function using a Gaussian process. This provides significant gains in computational efficiency.

Both asymptotically exact and inexact algorithms require careful tuning in order to provide good approximations in a reasonable amount of time. For instance, the DMH algorithm requires users to decide the length  $m$  of the inner sampler for generating an auxiliary variable. As  $m$  grows large the auxiliary variable becomes approximately a draw from the probability model at the expense of longer computing time. The function emulation algorithm requires users to select (1) an appropriate number  $d$  of particles to cover the important region of the parameter space, and (2) the sample size  $L$  for approximating the likelihood normalising function (or full likelihood function) at each particle. However, currently there is little guidance on how to tune these algorithms, and most of them rely on simulation studies. Also, the behavior of the algorithm varies across models or across datasets for a given model.

### **3 The need for diagnostics for intractable normalising function problems**

There is a vast literature on MCMC convergence diagnostics (see Cowles and Carlin, 1996; Flegal and Jones, 2011; Roy, 2020, for reviews). However, these diagnostics may not be adequate for asymptotically inexact algorithms. Suppose we have a sample generated by an asymptotically inexact method. Such a sample may not have an asymptotic distribution, or said sample may converge but to a mere approximation of the target distribution. Standard

MCMC diagnostics assess whether the sample has converged to its asymptotic distribution but do not assess whether the asymptotic distribution is equal to the target distribution. As discussed in Section 2, however, asymptotically exact algorithms for models with intractable normalising functions are available only for a few special cases, and even for these cases computing tends to be quite burdensome.

A number of approaches based on measuring the difference between sample means and target expectations have been proposed for assessing the quality of approximations provided by asymptotically inexact algorithms. Fan et al. (2006) proposed score function diagnostics for assessing estimates of some quantities the values of which are known under the target distribution. They suggested plotting the Monte Carlo estimate versus the sample size together with error bounds. Gorham and Mackey (2015) pointed out limitations of the score function diagnostics caused by considering only a finite class of functions and introduced a new diagnostic method based on a Stein discrepancy. Gorham and Mackey (2015) defined Stein discrepancies that bound the discrepancy between the sample mean and the target expectation over a large collection of functions whose target expectations are zero. The Stein discrepancies are supported by a theory of weak convergence and are attainable by solving a linear program. Combining this idea with the theory of reproducing kernels, Gorham and Mackey (2017) provided a closed-form kernel Stein discrepancy with sound theoretical support analogous to that of Gorham and Mackey (2015) (see Section 5.1 for details). These approaches are useful for comparing asymptotically approximate samplers and for selecting tuning parameters for such samplers. However, all of them require evaluating the score function of the target density, which is not possible for doubly intractable

posterior distributions. In contrast, our approaches apply broadly to asymptotically exact and inexact algorithms even for such challenging problems. To our knowledge, no other diagnostics are currently available for asymptotically inexact algorithms for models with intractable normalising functions. We have studied our diagnostics as applied in several challenging real data settings. In addition, we are able to provide some theoretical justification for our methods.

## 4 A curvature diagnostic

In this section we introduce two new diagnostics that are useful for tuning asymptotically exact and inexact algorithms: a curvature diagnostic (CD) and an approximate curvature diagnostic (ACD). The curvature diagnostic is based on the second Bartlett identity from the classical theory of maximum likelihood. The approximate curvature diagnostic is an approximation of the CD that is suitable for intractable normalising function problems.

### 4.1 A general purpose curvature diagnostic

Consider a sequence of sample points  $\boldsymbol{\theta}^{(1)}, \dots, \boldsymbol{\theta}^{(n)}$  generated by an algorithm having  $\pi(\boldsymbol{\theta} \mid \boldsymbol{x})$  as its target distribution. Our aim is to determine whether the sample will produce a good approximation to some quantity of interest, e.g.,  $E_{\pi}\{z(\boldsymbol{\theta})\}$ . One possible approach is to use functions whose expectations are known under the target distribution. One such function is the score function, which has expectation zero by the first Bartlett identity. Based on this, Fan et al. (2006) proposed the score function diagnostic described in Section 3. Our diagnostic, the curvature diagnostic, is inspired by the method for ob-

taining the asymptotic variance of a maximum likelihood estimator under a misspecified model. When the model is misspecified, the second Bartlett identity does not hold, which is to say (see details below) the sensitivity matrix is not equal to the variability matrix. And so the asymptotic variance of the estimator does not simplify to the inverse of the Fisher information. Our curvature diagnostic uses the dissimilarity between the sensitivity matrix and the variability matrix to assess the quality of the sample. If the asymptotic distribution of the sample is equal to the target distribution, these two estimated matrices are asymptotically equal. We provide details in the following paragraph.

The posterior density  $\pi(\boldsymbol{\theta} \mid \mathbf{x})$  has the sensitivity matrix

$$\mathcal{H}(\mathbf{x}) = \mathbb{E}_\pi \left\{ -\frac{\partial}{\partial \boldsymbol{\theta}} \mathbf{u}(\boldsymbol{\theta}) \right\} = \int_{\Theta} -\frac{\partial}{\partial \boldsymbol{\theta}} \mathbf{u}(\boldsymbol{\theta}) \pi(\boldsymbol{\theta} \mid \mathbf{x}) d\boldsymbol{\theta}$$

and the variability matrix

$$\mathcal{J}(\mathbf{x}) = \text{var}_\pi \{ \mathbf{u}(\boldsymbol{\theta}) \} = \mathbb{E}_\pi \{ \mathbf{u}(\boldsymbol{\theta}) \mathbf{u}(\boldsymbol{\theta})^\top \}, \quad (1)$$

where  $\mathbf{u}(\boldsymbol{\theta}) = \nabla_{\boldsymbol{\theta}} \log \pi(\boldsymbol{\theta} \mid \mathbf{x})$  is the score function of the posterior density and the second equation of (1) follows from Bartlett's first identity:  $\mathbb{E}_\pi \{ \mathbf{u}(\boldsymbol{\theta}) \} = \mathbf{0}$ . Let  $H(\boldsymbol{\theta}) = \frac{\partial}{\partial \boldsymbol{\theta}} \mathbf{u}(\boldsymbol{\theta})$  and  $J(\boldsymbol{\theta}) = \mathbf{u}(\boldsymbol{\theta}) \mathbf{u}(\boldsymbol{\theta})^\top$ . Using the sample  $\boldsymbol{\theta}^{(1)}, \dots, \boldsymbol{\theta}^{(n)}$  we construct Monte Carlo approximations to  $\mathcal{H}(\mathbf{x})$  and  $\mathcal{J}(\mathbf{x})$ , respectively, as

$$\mathcal{H}_n(\mathbf{x}) = \frac{1}{n} \sum_{i=1}^n -H(\boldsymbol{\theta}^{(i)}) \quad (2)$$

and

$$\mathcal{J}_n(\mathbf{x}) = \frac{1}{n} \sum_{i=1}^n J(\boldsymbol{\theta}^{(i)}). \quad (3)$$

By the ergodic theorem, if the asymptotic distribution of the sample is equal to the target distribution,  $\mathcal{H}_n(\mathbf{x})$  and  $\mathcal{J}_n(\mathbf{x})$  converge to  $\mathcal{H}(\mathbf{x})$  and  $\mathcal{J}(\mathbf{x})$ , respectively, almost surely as  $n \rightarrow \infty$ . Thus  $\mathcal{H}_n(\mathbf{x})$  and  $\mathcal{J}_n(\mathbf{x})$  are asymptotically equal by the second Bartlett identity. Dissimilarity between  $\mathcal{H}_n(\mathbf{x})$  and  $\mathcal{J}_n(\mathbf{x})$  can signal poor sample quality. We employ the following naive curvature diagnostic to measure the distance between the two matrices.

**Definition 1 (Naive Curvature Diagnostic)** *Consider a sample  $\boldsymbol{\theta}^{(1)}, \dots, \boldsymbol{\theta}^{(n)}$  generated by an algorithm having  $\pi(\boldsymbol{\theta} \mid \mathbf{x})$  as its target. Let  $\mathcal{H}_n(\mathbf{x})$  and  $\mathcal{J}_n(\mathbf{x})$  be Monte Carlo approximations, computed using the sample, to the sensitivity and variability matrices, respectively, of the target density. For any matrix norm  $\|\cdot\|$  a naive curvature diagnostic can be defined as*

$$\mathcal{N}_n(\mathbf{x}) := \|\mathcal{H}_n(\mathbf{x}) - \mathcal{J}_n(\mathbf{x})\|,$$

and  $\mathcal{N}_n(\mathbf{x}) \rightarrow 0$  almost surely as  $n \rightarrow \infty$  if the asymptotic distribution of the sample is equal to the target distribution.

The naive curvature diagnostic is useful for comparing the performances of different algorithms or performances of the same algorithm for different choices of tuning parameters. However,  $\mathcal{N}_n(\mathbf{x})$  is not bounded above, and its scale varies depending on the model or dataset being considered. This can make it difficult to interpret results. To aid interpretation we propose a scaling based on polar coordinates. Said formulation bounds the

curvature diagnostic between 0 and 1. The scaled version of the curvature diagnostic is defined as follows.

**Definition 2 (Scaled Curvature Diagnostic (CD))** Consider a sample  $\boldsymbol{\theta}^{(1)}, \dots, \boldsymbol{\theta}^{(n)}$  generated by an algorithm having  $\pi(\boldsymbol{\theta} \mid \mathbf{x})$  as its target. Let  $\mathcal{H}_n(\mathbf{x})$  and  $\mathcal{J}_n(\mathbf{x})$  be Monte Carlo approximations to the sensitivity and variability matrices of the target distribution. Let  $\mathbf{h}_n$  and  $\mathbf{j}_n$  denote the half-vectorizations of  $\mathcal{H}_n(\mathbf{x})$  and  $\mathcal{J}_n(\mathbf{x})$ , respectively, i.e.,  $\mathbf{h}_n = \text{vech}\{\mathcal{H}_n(\mathbf{x})\}$  and  $\mathbf{j}_n = \text{vech}\{\mathcal{J}_n(\mathbf{x})\}$ . For a scalar weight  $w \in (0, 1)$ , define the scaled curvature diagnostic as

$$\mathcal{C}_n(\mathbf{x}) := 1 - \left\{ w \cos(\mathbf{h}_n, \mathbf{j}_n) + (1 - w) \left( \frac{\|\mathbf{h}_n\|}{\|\mathbf{j}_n\|} \mathbb{1}_{\{\|\mathbf{h}_n\| \leq \|\mathbf{j}_n\|\}} + \frac{\|\mathbf{j}_n\|}{\|\mathbf{h}_n\|} \mathbb{1}_{\{\|\mathbf{h}_n\| > \|\mathbf{j}_n\|\}} \right) \right\},$$

where  $\cos(\mathbf{u}, \mathbf{v})$  denotes the cosine of the angle between vectors  $\mathbf{u}$  and  $\mathbf{v}$ . Then  $\mathcal{C}_n(\mathbf{x}) \rightarrow 0$  almost surely as  $n \rightarrow \infty$  if the asymptotic distribution of the sample is equal to the target distribution.

In the above definition  $\cos(\mathbf{h}_n, \mathbf{j}_n)$  is equal to 1 if the two vectors point in the same direction and decreases as the angle between the vectors increases. And  $(\|\mathbf{h}_n\|/\|\mathbf{j}_n\| \mathbb{1}_{\{\|\mathbf{h}_n\| \leq \|\mathbf{j}_n\|\}} + \|\mathbf{j}_n\|/\|\mathbf{h}_n\| \mathbb{1}_{\{\|\mathbf{h}_n\| > \|\mathbf{j}_n\|\}})$  is the ratio of a smaller norm to a larger norm. This quantity is equal to 1 if the two vectors have the same length and decreases toward 0 as the vectors' lengths diverge. The scaled curvature diagnostic  $\mathcal{C}_n(\mathbf{x})$  is obtained by computing the weighted sum of the two measures and subtracting from 1. Clearly,  $\mathcal{C}_n(\mathbf{x})$  is 0 if and only if  $\mathcal{H}_n(\mathbf{x})$  and  $\mathcal{J}_n(\mathbf{x})$  are equal. In the sequel we take  $w = 0.5$  and refer to the scaled curvature diagnostic as the curvature diagnostic.

## 4.2 An approximate curvature diagnostic for intractable normalising function problems

If the normalising function  $c(\boldsymbol{\theta})$  of the likelihood is intractable, it is not possible to evaluate the curvature diagnostic since the diagnostic involves  $\nabla_{\boldsymbol{\theta}} \log c(\boldsymbol{\theta})$ ,  $\{\nabla_{\boldsymbol{\theta}} \log c(\boldsymbol{\theta})\} \{\nabla_{\boldsymbol{\theta}} \log c(\boldsymbol{\theta})\}^{\top}$ , and  $\frac{\partial}{\partial \boldsymbol{\theta}} \{\nabla_{\boldsymbol{\theta}} \log c(\boldsymbol{\theta})\}$ . We therefore employ Monte Carlo approximations. To do this, we write the  $k$ th entry of the vector  $\nabla_{\boldsymbol{\theta}} \log c(\boldsymbol{\theta})$  as an expectation with respect to the model distribution:

$$\frac{\partial \log c(\boldsymbol{\theta})}{\partial \theta_k} = \mathbb{E}_f \left\{ \frac{\partial \log h(\mathbf{X}|\boldsymbol{\theta})}{\partial \theta_k} \right\}, \quad k = 1, \dots, p. \quad (4)$$

The derivation of (4) can be found in the supplementary materials. We approximate (4) using a sample generated from the model distribution:

$$\frac{\partial \log c(\boldsymbol{\theta})}{\partial \theta_k} \approx \frac{1}{2N} \sum_{j=1}^{2N} \frac{\partial \log h(\mathbf{y}^{(j)}|\boldsymbol{\theta})}{\partial \theta_k}, \quad (5)$$

where  $\mathbf{y}^{(1)}, \dots, \mathbf{y}^{(2N)}$  are auxiliary variables generated exactly from  $f(\cdot | \boldsymbol{\theta})$  or generated by a Monte Carlo algorithm having  $f(\cdot | \boldsymbol{\theta})$  as its target distribution. In a similar fashion, the unbiased approximation of the  $(k, l)$ th entry of  $\{\nabla_{\boldsymbol{\theta}} \log c(\boldsymbol{\theta})\} \{\nabla_{\boldsymbol{\theta}} \log c(\boldsymbol{\theta})\}^{\top}$  is calculated as

$$\frac{\partial \log c(\boldsymbol{\theta})}{\partial \theta_k} \frac{\partial \log c(\boldsymbol{\theta})}{\partial \theta_l} \approx \left\{ \frac{1}{N} \sum_{j=1}^N \frac{\partial \log h(\mathbf{y}^{(j)}|\boldsymbol{\theta})}{\partial \theta_k} \right\} \left\{ \frac{1}{N} \sum_{j=N+1}^{2N} \frac{\partial \log h(\mathbf{y}^{(j)}|\boldsymbol{\theta})}{\partial \theta_l} \right\},$$

where  $\mathbf{y}^{(1)}, \dots, \mathbf{y}^{(N)}$  and  $\mathbf{y}^{(N+1)}, \dots, \mathbf{y}^{(2N)}$  are independent sets of auxiliary variables generated from  $f(\cdot | \boldsymbol{\theta})$ . The two independent sets of sample points are needed to obtain an unbiased approximation to the product of two expectations. Finally, to approximate  $\frac{\partial}{\partial \boldsymbol{\theta}} \{\nabla_{\boldsymbol{\theta}} \log c(\boldsymbol{\theta})\}$  we write its  $(k, l)$ th entry as an expectation with respect to the model distribution:

$$\begin{aligned} \frac{\partial^2 \log c(\boldsymbol{\theta})}{\partial \theta_k \partial \theta_l} &= \mathbb{E}_f \left\{ \frac{\partial^2 \log h(\mathbf{X} | \boldsymbol{\theta})}{\partial \theta_k \partial \theta_l} \right\} + \mathbb{E}_f \left\{ \frac{\partial \log h(\mathbf{X} | \boldsymbol{\theta})}{\partial \theta_k} \frac{\partial \log h(\mathbf{X} | \boldsymbol{\theta})}{\partial \theta_l} \right\} \\ &\quad - \mathbb{E}_f \left\{ \frac{\partial \log h(\mathbf{X} | \boldsymbol{\theta})}{\partial \theta_k} \right\} \mathbb{E}_f \left\{ \frac{\partial \log h(\mathbf{X} | \boldsymbol{\theta})}{\partial \theta_l} \right\}. \end{aligned} \quad (6)$$

The derivation of (6) can be found in the supplementary materials. This leads to the unbiased approximation

$$\begin{aligned} \frac{\partial^2 \log c(\boldsymbol{\theta})}{\partial \theta_k \partial \theta_l} &\approx \frac{1}{2N} \sum_{j=1}^{2N} \frac{\partial^2 \log h(\mathbf{y}^{(j)} | \boldsymbol{\theta})}{\partial \theta_k \partial \theta_l} + \frac{1}{2N} \sum_{j=1}^{2N} \frac{\partial \log h(\mathbf{y}^{(j)} | \boldsymbol{\theta})}{\partial \theta_k} \frac{\partial \log h(\mathbf{y}^{(j)} | \boldsymbol{\theta})}{\partial \theta_l} \\ &\quad - \left\{ \frac{1}{N} \sum_{j=1}^N \frac{\partial \log h(\mathbf{y}^{(j)} | \boldsymbol{\theta})}{\partial \theta_k} \right\} \left\{ \frac{1}{N} \sum_{j=N+1}^{2N} \frac{\partial \log h(\mathbf{y}^{(j)} | \boldsymbol{\theta})}{\partial \theta_l} \right\}, \quad k, l = 1, \dots, p, \end{aligned}$$

for the independent sets of auxiliary variables  $\mathbf{y}^{(1)}, \dots, \mathbf{y}^{(N)}$  and  $\mathbf{y}^{(N+1)}, \dots, \mathbf{y}^{(2N)}$ . By plugging these approximations into  $H(\boldsymbol{\theta})$  and  $J(\boldsymbol{\theta})$ , we obtain their approximations  $\hat{H}_N(\boldsymbol{\theta})$  and  $\hat{J}_N(\boldsymbol{\theta})$ . We replace  $H(\boldsymbol{\theta})$  and  $J(\boldsymbol{\theta})$  with their approximations in (2) and (3) and obtain second-stage approximations  $\hat{\mathcal{H}}_{n,N}(\mathbf{x})$  and  $\hat{\mathcal{J}}_{n,N}(\mathbf{x})$  to the sensitivity and the variability matrices, respectively. An approximate version of the curvature diagnostic for intractable normalising function problems can be defined as follows.

**Definition 3 (Approximate Curvature Diagnostic (ACD))** Consider a sample  $\boldsymbol{\theta}^{(1)}, \dots, \boldsymbol{\theta}^{(n)}$  generated by an algorithm having  $\pi(\boldsymbol{\theta} \mid \mathbf{x})$  as its target. Consider two independent sets of auxiliary variables  $\mathbf{y}^{(1)}, \dots, \mathbf{y}^{(N)}$  and  $\mathbf{y}^{(N+1)}, \dots, \mathbf{y}^{(2N)}$  generated from the model distribution. Let  $\hat{\mathcal{H}}_{n,N}(\mathbf{x})$  and  $\hat{\mathcal{J}}_{n,N}(\mathbf{x})$  be two-stage Monte Carlo approximations, computed with the sample and the auxiliary variables, to the sensitivity and the variability matrices, respectively, of the target density. Let  $\hat{\mathbf{h}}_{n,N}$  and  $\hat{\mathbf{j}}_{n,N}$  denote half-vectorizations of  $\hat{\mathcal{H}}_{n,N}(\mathbf{x})$  and  $\hat{\mathcal{J}}_{n,N}(\mathbf{x})$ , respectively, i.e.,  $\hat{\mathbf{h}}_{n,N} = \text{vech}\{\hat{\mathcal{H}}_{n,N}(\mathbf{x})\}$  and  $\hat{\mathbf{j}}_{n,N} = \text{vech}\{\hat{\mathcal{J}}_{n,N}(\mathbf{x})\}$ . For a scalar weight  $w \in (0, 1)$ , an approximate curvature diagnostic can be defined as

$$\hat{C}_{n,N}(\mathbf{x}) := 1 - \left\{ w \cos(\hat{\mathbf{h}}_{n,N}, \hat{\mathbf{j}}_{n,N}) + (1 - w) \left( \frac{\|\hat{\mathbf{h}}_{n,N}\|}{\|\hat{\mathbf{j}}_{n,N}\|} \mathbb{1}_{\{\|\hat{\mathbf{h}}_{n,N}\| \leq \|\hat{\mathbf{j}}_{n,N}\|\}} + \frac{\|\hat{\mathbf{j}}_{n,N}\|}{\|\hat{\mathbf{h}}_{n,N}\|} \mathbb{1}_{\{\|\hat{\mathbf{h}}_{n,N}\| > \|\hat{\mathbf{j}}_{n,N}\|\}} \right) \right\}.$$

To provide theoretical justification for this diagnostic, we make the following assumptions regarding the prior density  $p(\boldsymbol{\theta})$  and the unnormalised probability model density  $h(\mathbf{x} \mid \boldsymbol{\theta})$ .

**Assumption 1** There exists  $c_p$  such that  $\|\nabla_{\boldsymbol{\theta}} \log p(\boldsymbol{\theta})\|_{\infty} \leq c_p$ .

**Assumption 2** There exists  $c_h$  such that  $\|\nabla_{\boldsymbol{\theta}} \log h(\mathbf{x} \mid \boldsymbol{\theta})\|_{\infty} \leq c_h$ .

Since the prior density is determined by the user, the prior's score function may be assumed to be bounded. In many applications Assumption 2 may be checked easily; this is the case for the examples discussed in Section 6. Under these assumptions, Theorem 1 quantifies the distance between the sensitivity matrix  $\mathcal{H}(\mathbf{x})$  and its two-stage approximation  $\hat{\mathcal{H}}_{n,N}(\mathbf{x})$  and the distance between the variability matrix  $\mathcal{J}(\mathbf{x})$  and its two-stage approximation  $\hat{\mathcal{J}}_{n,N}(\mathbf{x})$ .

**Theorem 1** Consider a sample  $\boldsymbol{\theta}^{(1)}, \dots, \boldsymbol{\theta}^{(n)}$  generated by an algorithm having  $\pi(\boldsymbol{\theta} \mid \mathbf{x})$  as its target. Suppose Assumptions 1 and 2 hold. If the asymptotic distribution of the sample

is equal to the target distribution, we have

$$\|\hat{\mathcal{H}}_{N,n}(\mathbf{x}) - \mathcal{H}(\mathbf{x})\|_{\infty} \leq \delta_1(n) + 2(1 + c_h)\epsilon(N)$$

and

$$\|\hat{\mathcal{J}}_{N,n}(\mathbf{x}) - \mathcal{J}(\mathbf{x})\|_{\infty} \leq \delta_2(n) + 2(2c_h + c_p)\epsilon(N)$$

almost surely.

A proof of Theorem 1 is provided in the supplementary materials. Provided the theorem holds, the two-stage approximations will get closer to their true values as the auxiliary sample size  $N$  and the posterior sample size  $n$  increase— $\delta_1(n)$  and  $\delta_2(n)$  go to 0 as  $n$  increases, and  $\epsilon(N)$  goes to 0 as  $N$  increases. Thus if the asymptotic distribution of the sample is equal to the target distribution, the approximate curvature diagnostic  $\hat{\mathcal{C}}_{n,N}(\mathbf{x})$  goes to 0 as  $n$  and  $N$  increase. With  $N = 100,000$ , ACD well approximates CD, as is evident in an example provided in the supplementary materials. Thus we set  $N = 100,000$  for the remainder of this article.

## 5 A kernel Stein discrepancy

In this section we briefly describe an inverse multiquadric kernel Stein discrepancy (IMQ KSD) introduced by Gorham and Mackey (2017) and develop a Monte Carlo approximate version, AIKS (approximate inverse multiquadric kernel Stein discrepancy), for use with

doubly intractable target distributions. IMQ KSD is a kernel Stein discrepancy-based diagnostic that has theoretical support and is available in closed form. To make this approach available for models with intractable normalising functions, we develop its Monte Carlo approximation and show that AIKS asymptotically inherits the same convergence properties as IMQ KSD.

## 5.1 An inverse multiquadric kernel Stein discrepancy

Gorham and Mackey (2017) defined the inverse multiquadric kernel Stein discrepancy for assessing the quality of a sample and provided theoretical justification for its use in diagnosing convergence of a sequence of sample points to a target distribution. Consider a target distribution  $P$  with probability density function  $\pi(\boldsymbol{\theta})$  under which direct integration is infeasible. Consider a weighted sample targeting  $P$ , which is defined as  $Q_n = \sum_{i=1}^n q_n(\boldsymbol{\theta}^{(i)})\delta_{\boldsymbol{\theta}^{(i)}}$  with sample points  $\boldsymbol{\theta}^{(1)}, \dots, \boldsymbol{\theta}^{(n)}$  and probability mass function  $q_n$ . Suppose we want to evaluate  $E_P\{z(\boldsymbol{\theta})\}$ , which is intractable. The weighted sample  $Q_n$  provides an approximation  $E_{Q_n}\{z(\boldsymbol{\theta})\} = \sum_{i=1}^n z(\boldsymbol{\theta}^{(i)})q_n(\boldsymbol{\theta}^{(i)})$  of the target expectation. To assess the quality of the approximation, one may consider discrepancies quantifying the maximum expectation error over a set of test functions  $\mathcal{Z}$ :

$$d_{\mathcal{Z}}(Q_n, P) = \sup_{z \in \mathcal{Z}} |E_P\{z(\boldsymbol{\theta})\} - E_{Q_n}\{z(\boldsymbol{\theta})\}|.$$

When  $\mathcal{Z}$  is large enough the discrepancy is called an integral probability metric (IPM) (Müller, 1997) and  $d_{\mathcal{Z}}(Q_n, P) \rightarrow 0$  only if  $Q_n \Rightarrow P$  for any sequence  $Q_n$ . We use  $\Rightarrow$  to denote the weak convergence of a sequence of probability measures. However, it is not

practical to use IPM for assessing a sample since  $E_P \{z(\boldsymbol{\theta})\}$  may not be computable for some  $z \in \mathcal{Z}$ .

According to Stein's method (Stein, 1972), Gorham and Mackey (2015) defined a Stein discrepancy as

$$\mathcal{S}(Q_n, \mathcal{T}, \mathcal{G}) = \sup_{g \in \mathcal{G}} |E_{Q_n} \{(\mathcal{T}g)(\boldsymbol{\theta})\}|$$

for a Stein operator  $\mathcal{T}$  and a Stein set  $\mathcal{G}$  that satisfy  $E_P \{(\mathcal{T}g)(\boldsymbol{\theta})\} = 0$  for all  $g \in \mathcal{G}$ . The Stein discrepancy is the maximum expectation error over the Stein set  $\mathcal{G}$  given the Stein operator  $\mathcal{T}$ . This avoids explicit integration under  $P$  by selecting appropriate  $\mathcal{T}$  and  $\mathcal{G}$  that lead the target expectation to zero. Gorham and Mackey (2017) selected Langevin Stein operator and kernel Stein set based on the inverse multiquadric kernel and defined the inverse multiquadric kernel Stein discrepancy  $\mathcal{S}(Q_n, \mathcal{T}_P, \mathcal{G}_{k, \|\cdot\|})$  for any norm  $\|\cdot\|$ , which admits closed-form solution.

**Definition 4 (Inverse Multiquadric Kernel Stein Discrepancy (IMQ KSD) (Gorham and Mackey, 2017))**

*Let  $k(\mathbf{x}, \mathbf{y}) = (c^2 + \|\mathbf{x} - \mathbf{y}\|_2^2)^\beta$  for some  $c > 0$  and  $\beta \in (-1, 0)$ . For each  $j \in \{1, \dots, p\}$  construct the Stein kernel*

$$k_0^j(\mathbf{x}, \mathbf{y}) = u_j(\mathbf{x})u_j(\mathbf{y})k(\mathbf{x}, \mathbf{y}) + u_j(\mathbf{x})\nabla_{y_j}k(\mathbf{x}, \mathbf{y}) + u_j(\mathbf{y})\nabla_{x_j}k(\mathbf{x}, \mathbf{y}) + \nabla_{x_j}\nabla_{y_j}k(\mathbf{x}, \mathbf{y}),$$

*where  $u_j$  is the  $j$ th entry of the score function of the target density. Then IMQ KSD*

$\mathcal{S}(Q_n, \mathcal{T}_P, \mathcal{G}_{k, \|\cdot\|}) = \|\mathbf{w}\|$ , where

$$w_j = \sqrt{\sum_{k,l=1}^n q_n(\boldsymbol{\theta}^{(k)}) k_0^j(\boldsymbol{\theta}^{(k)}, \boldsymbol{\theta}^{(l)}) q_n(\boldsymbol{\theta}^{(l)})}.$$

Computation of  $\mathbf{w}$  is parallelizable over sample pairs  $(\boldsymbol{\theta}^{(k)}, \boldsymbol{\theta}^{(l)})$  and coordinates  $j$ . For a target distribution with constrained support  $[\ell_1, u_1] \times \cdots \times [\ell_d, u_d]$ , Gorham and Mackey (2017) suggest using the following kernel that respects these constraints when computing the Stein kernel:

$$k_R(\mathbf{x}, \mathbf{y}) = k(\mathbf{x}, \mathbf{y}) \prod_{\{j: \ell_j > -\infty\}} (x_j - \ell_j)(y_j - \ell_j) \prod_{\{k: u_k < \infty\}} (x_k - u_k)(y_k - u_k).$$

Gorham and Mackey (2017) provided theoretical justification for its use for diagnosing convergence of a sequence  $Q_n$  to its target distribution  $P$ :

- (a) For a distantly dissipative target distribution  $P$ , if  $\mathcal{S}(Q_n, \mathcal{T}_P, \mathcal{G}_{k, \|\cdot\|}) \rightarrow 0$ , then  $Q_n \Rightarrow P$ .
- (b) For a target distribution  $P$  having Lipschitz score function with  $\mathbb{E}_P \{\|\mathbf{u}(\boldsymbol{\theta})\|_2^2\} < \infty$ , if the Wasserstein distance  $d_{\mathcal{W}_{\|\cdot\|_2}}(Q_n, P) \rightarrow 0$ , then  $\mathcal{S}(Q_n, \mathcal{T}_P, \mathcal{G}_{k, \|\cdot\|}) \rightarrow 0$ .

## 5.2 An approximate inverse multiquadric kernel Stein discrepancy for intractable normalising function problems

When the target distribution  $P$  is doubly intractable, computation of IMQ KSD is not feasible. This is because IMQ KSD requires evaluating the score function of the target

density. In this section we introduce an approximate version of IMQ KSD by replacing the score function with its Monte Carlo approximation. The approximate inverse multiquadric kernel Stein discrepancy is defined as follows.

**Definition 5 (Approximate Inverse Multiquadric Kernel Stein Discrepancy (AIKS))** *Let*

$k(\mathbf{x}, \mathbf{y}) = (c^2 + \|\mathbf{x} - \mathbf{y}\|_2^2)^\beta$  *for some*  $c > 0$  *and*  $\beta \in (-1, 0)$ . *For each*  $j \in \{1, \dots, p\}$  *define an approximate Stein kernel*

$$\hat{k}_0^j(\mathbf{x}, \mathbf{y}) = \hat{u}_j(\mathbf{x})\hat{u}_j(\mathbf{y})k(\mathbf{x}, \mathbf{y}) + \hat{u}_j(\mathbf{x})\nabla_{y_j}k(\mathbf{x}, \mathbf{y}) + \hat{u}_j(\mathbf{y})\nabla_{x_j}k(\mathbf{x}, \mathbf{y}) + \nabla_{x_j}\nabla_{y_j}k(\mathbf{x}, \mathbf{y}),$$

where  $\hat{u}_j$  is the  $j$ th entry of the approximate score function of the target density. Then

AIKS  $\hat{\mathcal{S}}(Q_n, \mathcal{T}_P, \mathcal{G}_{k, \|\cdot\|}) = \|\hat{\mathbf{w}}\|$ , where

$$\hat{w}_j = \sqrt{\sum_{k,l=1}^n q_n(\boldsymbol{\theta}^{(k)})\hat{k}_0^j(\boldsymbol{\theta}^{(k)}, \boldsymbol{\theta}^{(l)})q_n(\boldsymbol{\theta}^{(l)})}.$$

For doubly intractable target density  $\pi(\boldsymbol{\theta} \mid \mathbf{x})$ , the score function can be approximated using (5) from Section 4.2. Under the assumptions of IMQ KSD on the target distribution, Theorem 2 quantifies the distance between AIKS and IMQ KSD for any  $L^p$  norm.

**Theorem 2** *For a target distribution*  $P$  *having a bounded score function and a sample distribution*  $Q_n$  *targeting*  $P$ , *let*  $\mathcal{S}(Q_n, \mathcal{T}_P, \mathcal{G}_{k, \|\cdot\|_p})$  *and*  $\hat{\mathcal{S}}(Q_n, \mathcal{T}_P, \mathcal{G}_{k, \|\cdot\|_p})$  *denote IMQ KSD and AIKS, respectively, for the sample distribution. Then*

$$\left| \hat{\mathcal{S}}(Q_n, \mathcal{T}_P, \mathcal{G}_{k, \|\cdot\|_p}) - \mathcal{S}(Q_n, \mathcal{T}_P, \mathcal{G}_{k, \|\cdot\|_p}) \right| \leq \{n^2 M \epsilon(N)\}^{1/p}$$

*almost surely for bounded constant  $M$ , where  $N$  is the auxiliary sample size used to approximate the score function of the target density.*

A proof of Theorem 2 is provided in the supplementary materials. If the theorem holds, AIKS will get closer to IMQ KSD as the auxiliary sample size  $N$  increases— $\epsilon(N)$  goes to 0 as  $N$  increases. This implies that AIKS asymptotically inherits the same convergence properties as IMQ KSD for any  $L^p$  norm. In this article we use the  $L^2$  norm,  $\beta = -1/2$ , and  $c = 1$ . With  $N = 100,000$  AIKS provides a good approximation to IMQ KSD, as is evident from the example described in the supplementary materials. Thus we set  $N = 100,000$  for the rest of this article.

## 6 Applications

Here we apply our methods to both asymptotically exact and asymptotically inexact algorithms in the context of three general classes of models with intractable normalising functions: (1) the Ising model, (2) a social network model, and (3) an attraction-repulsion point process model. Effective sample size (ESS), which is one of the most widely used MCMC diagnostics, is helpful for asymptotically exact methods since all chains converge to the target distribution. However, for asymptotically inexact methods, ESS is inadequate since an algorithm that mixes better might yield a poorer approximation to the target distribution. Hence, to illustrate the usefulness of our approaches for asymptotically inexact methods, we compare the approximate curvature diagnostic (ACD) and the approximate multiquadric kernel Stein discrepancy (AIKS) with ESS. We note that application of our curvature diagnostic (CD) extends well beyond intractable normalising function problems.

CD is, in principle, applicable in most any likelihood-based context where misspecification is of concern. The code for our diagnostics is implemented in R (Ihaka and Gentleman, 1996) and C++, using the `Rcpp` and `RcppArmadillo` packages (Eddelbuettel and Francois, 2011). The calculation of ESS follows Kass et al. (1998) and Robert and Casella (2013). All code was run on dual 10 core Xeon E5-2680 processors on the Penn State high performance computing cluster. The source code may be found in the following repository (<https://github.com/bokgyeong/Diagnostics>).

## 6.1 The Ising model

The Ising model (Lenz, 1920; Ising, 1925) is one of the most famous and important models from statistical physics and provides an approach for modeling binary images. For an  $r \times s$  lattice  $\mathbf{x} = \{x_{ij}\}$  with binary values  $x_{i,j} \in \{-1, 1\}$ , where  $i, j$  denotes the row and column, the Ising model with a parameter  $\theta \in (0, 1)$  has likelihood

$$L(\theta \mid \mathbf{x}) = \frac{1}{c(\theta)} \exp\{\theta S(\mathbf{x})\},$$

where

$$S(\mathbf{x}) = \sum_{i=1}^r \sum_{j=1}^{s-1} x_{i,j} x_{i,j+1} + \sum_{i=1}^{r-1} \sum_{j=1}^s x_{i,j} x_{i+1,j},$$

is the sum over all possible products of neighboring elements and imposes spatial dependence. A larger value for the dependence parameter  $\theta$  produces stronger interactions among neighboring observations. Calculation of the normalising function  $c(\theta)$  requires summation over all  $2^{rs}$  possible outcomes for the model, which is computationally infeasible

even for lattices of moderate size. We carried out our simulation using perfect sampling (Propp and Wilson, 1996) on a  $30 \times 30$  lattice with the parameter setting  $\theta = 0.43$ , which represents strong dependence.

For this example we consider two algorithms: (1) Liang et al. (2016)’s adaptive exchange (AEX) algorithm, which is asymptotically exact, and (2) Liang (2010)’s double Metropolis–Hastings (DMH) algorithm, which is asymptotically inexact. The AEX algorithm runs two chains simultaneously: an auxiliary chain and a target chain. The auxiliary chain simulates a sample from a set of distributions,  $\{h(\mathbf{x} | \boldsymbol{\theta}^{(1)})/c(\boldsymbol{\theta}^{(1)}), \dots, h(\mathbf{x} | \boldsymbol{\theta}^{(d)})/c(\boldsymbol{\theta}^{(d)})\}$ , where  $\boldsymbol{\theta}^{(1)}, \dots, \boldsymbol{\theta}^{(d)}$  are predetermined particles over the parameter space, and stores the generated sample at each iteration. The target chain generates a posterior sample via the exchange algorithm (Murray et al., 2006), where an auxiliary variable  $\mathbf{y}$  is sampled from the cumulative samples in the auxiliary chain instead of exact sampling of  $\mathbf{y}$ . The DMH algorithm is asymptotically inexact but was found to be very efficient in terms of effective sample size per unit time and is applicable for doubly intractable problems with higher parameter dimension. DMH replaces the exact sampling of  $\mathbf{y}$  in the exchange algorithm with a standard Metropolis–Hastings algorithm, an “inner sampler,” at each iteration. To find appropriate values for the tuning parameters of the algorithms, we generate multiple chains from each algorithm with different choices of the tuning parameters. We implement AEX with different numbers  $d$  of particles, where particles are selected from fractional DMH, which is DMH with a larger acceptance probability. The choice of the other tuning parameters follows Park and Haran (2018). We implement DMH with different numbers  $m$  of (inner) Gibbs updates. We use a uniform prior with range  $[0, 1]$  for  $\theta$ . All algorithms

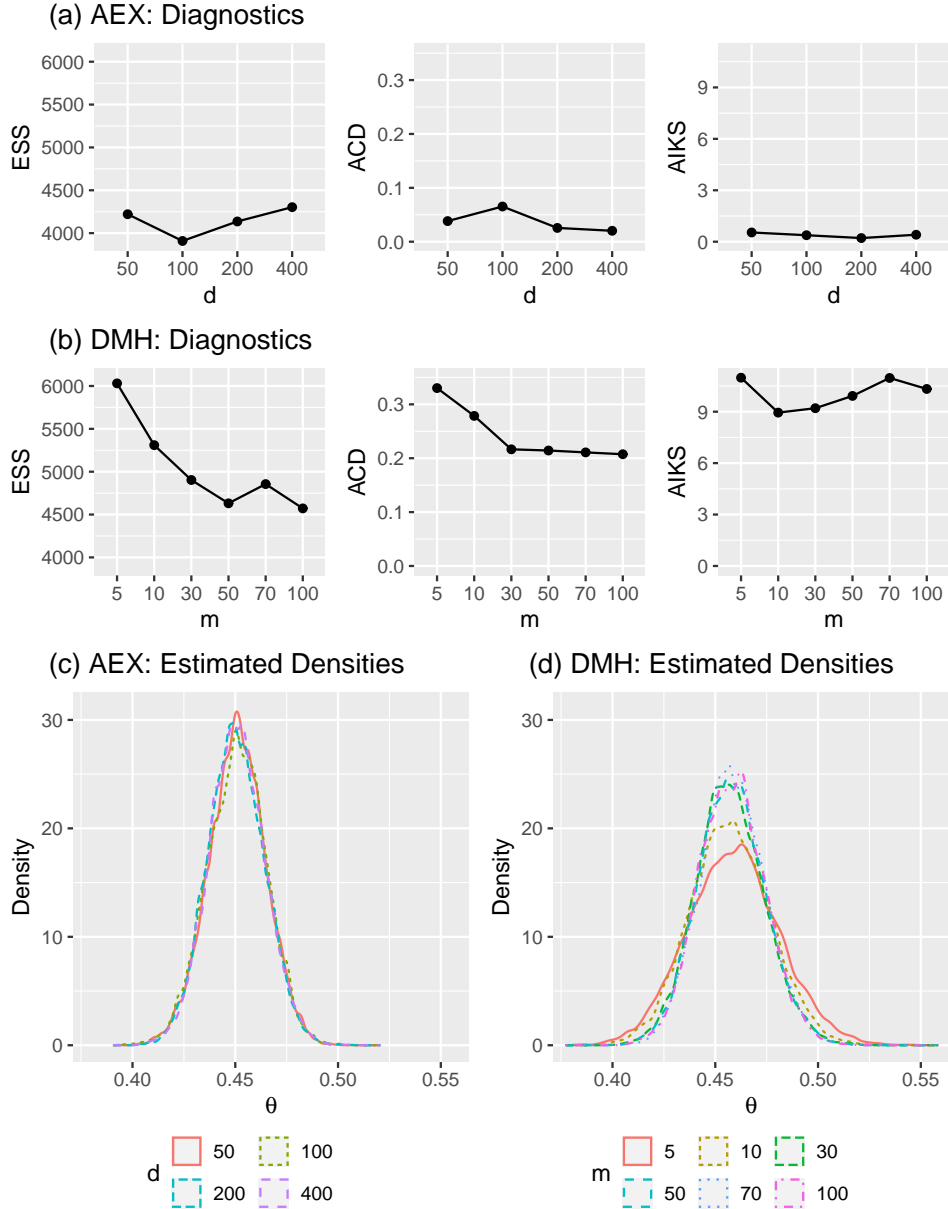


Figure 1: Results for a simulated binary lattice from the Ising model with  $\theta = 0.43$ . **(a)** Diagnostics (ESS, ACD, AIKS) applied to samples generated from AEX with different numbers  $d$  of particles. **(b)** Diagnostics applied to samples generated from DMH with different numbers  $m$  of (inner) Gibbs updates. **(c)** Estimated posterior densities for AEX samples. **(d)** Estimated posterior densities for DMH samples. A larger ESS is better, a smaller ACD is better, and a smaller AIKS is better. For AEX, all of diagnostics are similar for the different values of  $d$ . For DMH, ESS recommends  $m = 5$  and implies that DMH performs better than AEX. On the other hand, ACD and AIKS correctly indicate that the quality of DMH samples are poorer than that of AEX samples.

were run for 100,000 iterations.

ESS, ACD, and AIKS are calculated based on entire sample paths; there was no burn-in or thinning. When computing ACD and AIKS, two independent sets of  $N = 100,000$  auxiliary variables are generated via Gibbs sampling for approximating the score function,  $H$  matrix, and  $J$  matrix at each unique posterior sample point. We used parallel computing to obtain the approximations and to compute AIKS. For a posterior sample path, the approximation step took at most 3.7 hours. Given the approximations, the longest ACD computation took 20.2 seconds and the longest AIKS computation took 21.2 seconds.

Figure 1 (a) shows the diagnostic values for AEX for various values of  $d$ . The diagnostics have similar values across the  $d$  values, which implies that AEX is not so sensitive to the number of particles in this example. ESS and ACD are optimized at  $d = 400$ , for which ESS is 4303 and ACD is 0.020. The minimum of AIKS is 0.212 at  $d = 200$ . In Figure 1 (c) it is observed that the estimated posterior densities of the samples are so similar between different  $d$  values that it is difficult to distinguish them. For DMH, ACD and AIKS provide considerably different conclusions from ESS. Figure 1 (b) indicates that ESS is maximized (the best) at  $m = 5$  and generally decreases as  $m$  increases. The DMH samples have larger (better) ESS than any of the AEX samples (the maximum of ESS of the DMH samples is 6031). On the other hand, ACD takes its largest (worst) values at  $m = 5$  and decrease as  $m$  increases. AIKS has similar values across the  $m$  values. The minimum of ACD is 0.21 at  $m = 100$  and the minimum of AIKS is 8.95 at  $m = 10$ . Compared to the AEX samples, ACD and AIKS are large (worse) for the DMH samples. Figure 1 (d) shows that the DMH samples converge to a distribution as  $m$  increases. The estimated densities have

higher peaks and lighter tails as  $m$  increases. When  $m$  is 30 and above, they look similar to one another. Compared to the AEX samples, all the DMH samples have much lower peaks in their estimated densities. Considering the AEX sample with  $d = 400$  as our gold standard (AEX is asymptotically exact and ACD and AIKS are quite close to zero at  $d = 400$ ), this indicates that DMH does not work well even for a fairly large  $m$ . This shows that ACD and AIKS perform well in assessing how close samples are to the exact posterior. Not surprisingly, ESS is inadequate as a tool for this purpose. In summary, our approaches provide good guidance on how to assess the quality of samples for both the asymptotically exact and asymptotically inexact algorithms.

## 6.2 A social network model

An exponential family random graph model (ERGM) (Robins et al., 2007; Hunter et al., 2008) is a statistical model for analyzing network data. Consider an undirected ERGM with  $n$  vertices. Relationships among the vertices can be represented as an  $n \times n$  adjacency matrix  $\mathbf{x}$  as follows: for all  $i \neq j$ ,  $x_{i,j} = 1$  if the  $i$ th and  $j$ th vertices are connected, and  $x_{i,j} = 0$  otherwise. And  $x_{i,i}$  is 0 for all  $i \in \{1, \dots, n\}$ , i.e., there are no loops. The number of possible network configurations is  $2^{n(n-1)/2}$  and summation over those configurations is required to calculate the normalising function of the model. Thus computing  $c(\boldsymbol{\theta})$  is infeasible unless  $n$  is quite small.

For an undirected graph with  $n$  vertices, the ERGM likelihood is given by

$$L(\boldsymbol{\theta} \mid \mathbf{x}) = \frac{1}{c(\boldsymbol{\theta})} \exp\{\theta_1 S_1(\mathbf{x}) + \theta_2 S_2(\mathbf{x})\},$$

$$S_1(\mathbf{x}) = \sum_{i=1}^n \begin{pmatrix} x_{i+} \\ 1 \end{pmatrix},$$

$$S_2(\mathbf{x}) = e^\tau \sum_{k=1}^{n-2} \{1 - (1 - e^{-\tau})^k\} \text{EP}_k(\mathbf{x}).$$

The sufficient statistics  $S_1(\mathbf{x})$  and  $S_2(\mathbf{x})$  are the number of edges in the graph and the geometrically weighted edge-wise shared partnership (GWESP) statistic (Hunter and Handcock, 2006; Hunter, 2007), respectively.  $x_{i+}$  denotes the sum of the  $i$ th row of the adjacency matrix and  $\text{EP}_k(\mathbf{x})$  denotes the number of edges between two vertices that share exactly  $k$  neighbors. It is assumed that  $\tau$  is fixed at a value of 0.25. We simulated a network with 30 actors using 10,000 cycles of Gibbs updates, where the true parameter was  $\boldsymbol{\theta} = (\theta_1, \theta_2)^\top = (-0.96, 0.04)^\top$ .

For this example we consider two algorithms: (1) Atchadé et al. (2013)'s adaptive MCMC (ALR) algorithm, which is asymptotically exact, and (2) the DMH algorithm, which is asymptotically inexact. The ALR algorithm introduces multiple particles  $\boldsymbol{\theta}^{(1)}, \dots, \boldsymbol{\theta}^{(d)}$  over the parameter space and approximates  $c(\boldsymbol{\theta})$  in the Metropolis–Hastings acceptance probability using a linear combination of importance sampling estimates for  $c(\boldsymbol{\theta})/c(\boldsymbol{\theta}^{(1)}), \dots, c(\boldsymbol{\theta})/c(\boldsymbol{\theta}^{(d)})$ . We explained the DMH algorithm in Section 6.1. We generate multiple chains for each algorithm with different choices of the tuning parameters. We implement ALR with different numbers  $d$  of particles, where the particles are chosen from a short run of DMH with a

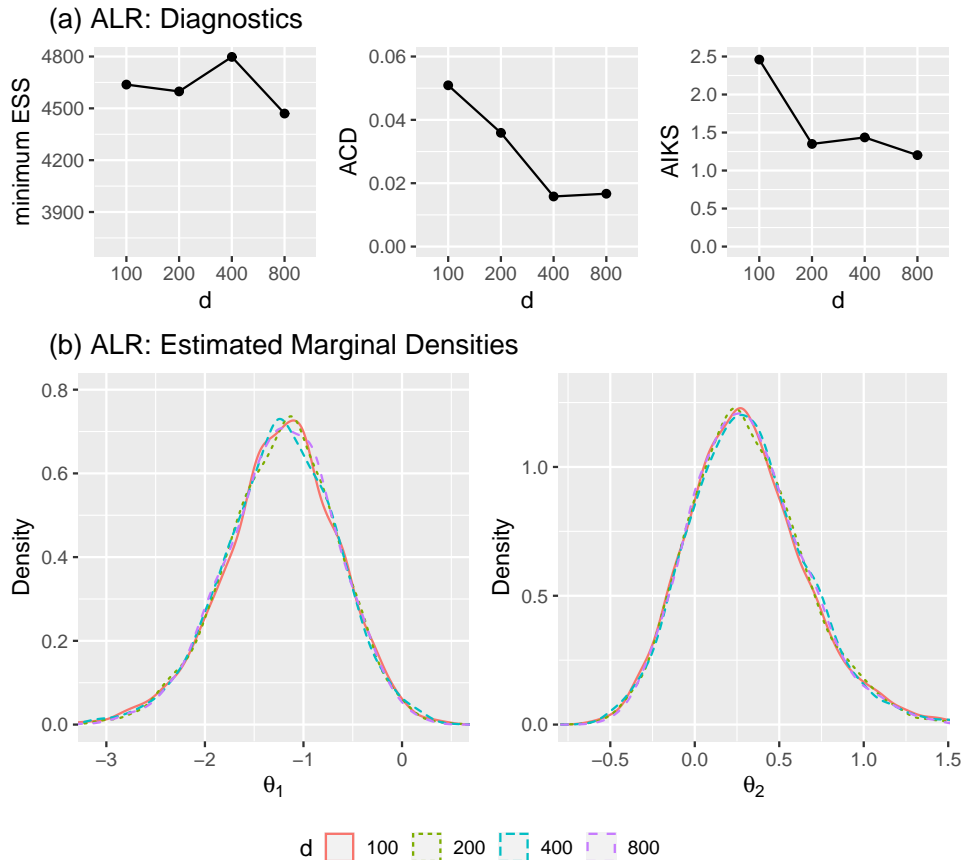


Figure 2: A simulated network from ERGM with  $\boldsymbol{\theta} = (\theta_1, \theta_2)^\top = (-0.96, 0.04)^\top$ . **(a)** Diagnostics (minimum ESS, ACD, AIKS) applied to samples generated from ALR with different numbers  $d$  of particles. A larger ESS is better, a smaller ACD is better, and a smaller AIKS is better. **(b)** Estimated marginal posterior densities of the samples. ACD and AIKS recommend  $d$  of 400 or more, while the minimum ESS is similar for the different values of  $d$ .

single cycle of (inner) Gibbs updates. The choice of other components to be tuned follows Park and Haran (2018). We also implement DMH with different numbers  $m$  of Gibbs updates. We use uniform priors with range  $[-5.00, 2.27] \times [-1.57, 2.32]$  for  $(\theta_1, \theta_2)^\top$ , which are centered around the maximum pseudo-likelihood estimates (MPLE) and have widths of 12 standard deviations. All algorithms were run for 100,000 iterations. To expedite computing we thinned the samples at equally spaced intervals of 20 to obtain 5,000 sample points. When computing ACD and AIKS, two independent sets of  $N = 100,000$  auxiliary variables

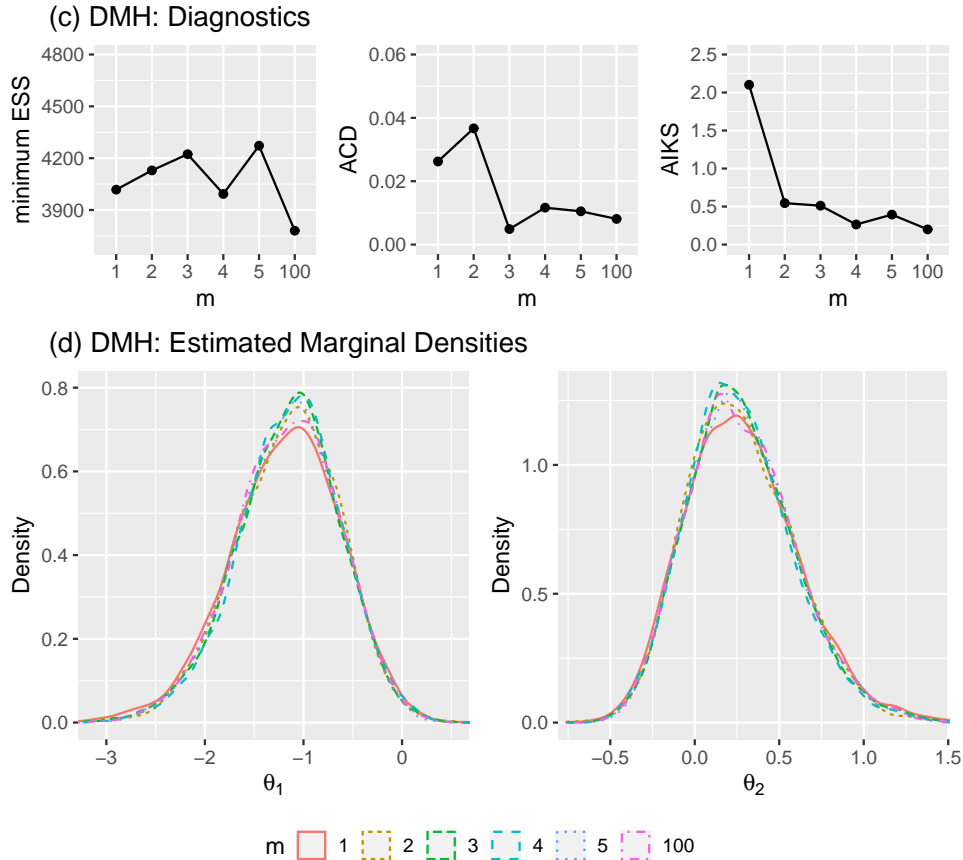


Figure 3: A simulated network from ERGM with  $\theta = (\theta_1, \theta_2)^\top = (-0.96, 0.04)^\top$ . (a) Diagnostics (minimum ESS, ACD, AIKS) applied to samples generated from DMH with different numbers  $m$  of (inner) Gibbs updates. A larger ESS is better, a smaller ACD is better, and a smaller AIKS is better. (b) Estimated marginal posterior densities of the samples. The minimum ESS recommends  $m = 5$  and does not recommend  $m = 100$ . ACD recommends  $m$  of at least 3 and AIKS recommends  $m$  of at least 2.

are generated via Gibbs sampling for approximating the score function,  $H$  matrix, and  $J$  matrix at each of the sample points. We used parallel computing to obtain the approximations and to compute AIKS. For a single posterior sample path the approximation step took at most 3.9 hours. Given the approximations, the longest ACD computation took 0.5 seconds and the longest AIKS computation took 0.85 seconds.

Figure 2 (a) shows minimum effective sample size, ACD, and AIKS for the ALR sample for an array of  $d$  values. The minimum ESS is pretty high at every choice of  $d$  (its maximum

is 4798 at  $d = 400$ ). Unlike ESS, ACD and AIKS generally decrease as  $d$  increases. ACD implies that  $d$  should be at least 400 (its minimum is 0.016 at  $d = 400$ ), and AIKS suggests that  $d$  should be at least 200 (its minimum is 1.203 at  $d = 800$ ). In Figure 2 (b), the estimated marginal posterior densities of the samples seem similar between different  $d$  values. For DMH, Figure 3 (a) shows that the minimum ESS is maximized (the best) at  $m = 5$  and minimized (the worst) at  $m = 100$  (it is 4272 at  $m = 5$  and 3780 at  $m = 100$ ). Compared to the ALR samples, the minimum ESS is relatively small (worse) for the DMH samples. ACD and AIKS provide significantly different conclusions from ESS. They imply that the DMH sample generally becomes better as  $m$  increases. ACD suggests that  $m$  should be at least 3 (its minimum is 0.005 at  $m = 3$ ), and AIKS implies that  $m$  should be at least 2 (its minimum is 0.2 at  $m = 100$ ). ACD and AIKS also imply that the DMH samples are better than any of the ALR samples when  $m$  is selected according to their guidance. In Figure 3 (b), we observe that the DMH sample with  $m = 1$  has slightly lower peaks in both of the estimated marginal posterior densities compared to the others. This is consistent with the result that ACD and AIKS provide relatively large values at  $m = 1$ . In summary, our approaches help compare performance between algorithms as well as tune algorithms. In particular, for asymptotically inexact algorithms, our methods can guide users to appropriately choose their tuning parameters and help provide reliable inference. In general it would be very difficult to compare the results of DMH across different values of  $m$ , as well as to compare DMH to ALR.

### 6.3 An attraction-repulsion point process model

Consider a realization of random points  $\mathbf{x} = \{x_1, \dots, x_n\}$  in a bounded plan  $S \subset \mathbb{R}^2$ . A probability model may be used to illustrate spatial patterns among the points by introducing an interaction function  $\phi(r_{i,j})$  where  $r_{i,j}$  is the distance between the coordinates of  $x_i$  and  $x_j$ . Strauss (1975) introduced Strauss process describing repulsion patterns among the points. Goldstein et al. (2015) extended the process and developed a point process to describe both attraction and repulsion patterns of the cells infected with human respiratory syncytial virus (RSV). The probability model with parameters  $\boldsymbol{\theta} = (\lambda, \theta_1, \theta_2, \theta_3)^\top$  is

$$L(\boldsymbol{\theta} | \mathbf{x}) = \frac{\lambda^n \prod_{i=1}^n \exp \left\{ \min \left( \sum_{i \neq j} \log \phi(r_{i,j}), 1.2 \right) \right\}}{c(\boldsymbol{\theta})},$$

and the interaction function is

$$\phi(r) = \begin{cases} 0 & 0 \leq r \leq R \\ \phi_1(r) = \theta_1 - \left\{ \frac{\sqrt{\theta_1}}{\theta_2 - R} (r - \theta_2) \right\}^2 & R < r \leq r_1 \\ \phi_2(r) = 1 + \frac{1}{\{\theta_3(r - r_2)\}^2} & r > r_1 \end{cases}$$

This model has four parameters:  $\lambda$  controls the intensity of the process and  $(\theta_1, \theta_2, \theta_3)$  determine the shape of the interaction function  $\phi$ .  $\theta_1$  is the value of  $\phi(\cdot)$  at its peak,  $\theta_2$  is the value of  $r$  at the peak, and  $\theta_3$  controls the descent rate after the peak.  $R$  is the minimum distance allowed between any two points, and  $r_1$  and  $r_2$  are solutions to the

system of equations

$$\begin{aligned}\phi_1(r_1) &= \phi_2(r_1) \\ \frac{d\phi_1(r_1)}{dr} &= \frac{d\phi_2(r_1)}{dr},\end{aligned}$$

which allows the interaction function to be continuously differentiable. In order to calculate the normalising function  $c(\boldsymbol{\theta})$  of the model, integration over the continuous domain  $S$  is required, which is infeasible. We study the point pattern of RSV data ( $n \approx 3000$ ) generated from the experimental setting of 1A2A-16h (the primary virus is RSV-A, the secondary virus is RSV-B, and there is a 16-hour time lag between the exposures).

For this example we consider the DMH algorithm and Park and Haran (2020)'s likelihood function emulation (LikEm) algorithm, both of which are asymptotically inexact. We have not implemented AEX and ALR because this model does not have summary statistics, which makes the algorithms impractical. LikEm algorithm estimates the likelihood function at prespecified particles  $\boldsymbol{\theta}^{(1)}, \dots, \boldsymbol{\theta}^{(d)}$  using importance sampling and approximates  $c(\boldsymbol{\theta})$  in the Metropolis–Hastings acceptance probability by fitting a Gaussian process to the importance sampling estimates. In order to find suitable values for the tuning parameters of these algorithms, we implement DMH with different numbers  $m$  of (inner) birth-death updates and LikEm with different numbers  $d$  of particles. The particles are selected from a short run of DMH with  $m = 30,000$ . We use a uniform prior distribution for  $(\lambda, \theta_1, \theta_2, \theta_3)$  with range  $[2 \times 10^{-4}, 6 \times 10^{-4}] \times [1, 2] \times [0, 20] \times [0, 1]$  which is plausible for this data (Goldstein et al., 2015). All algorithms were run until 50,000 iterations. To expedite com-

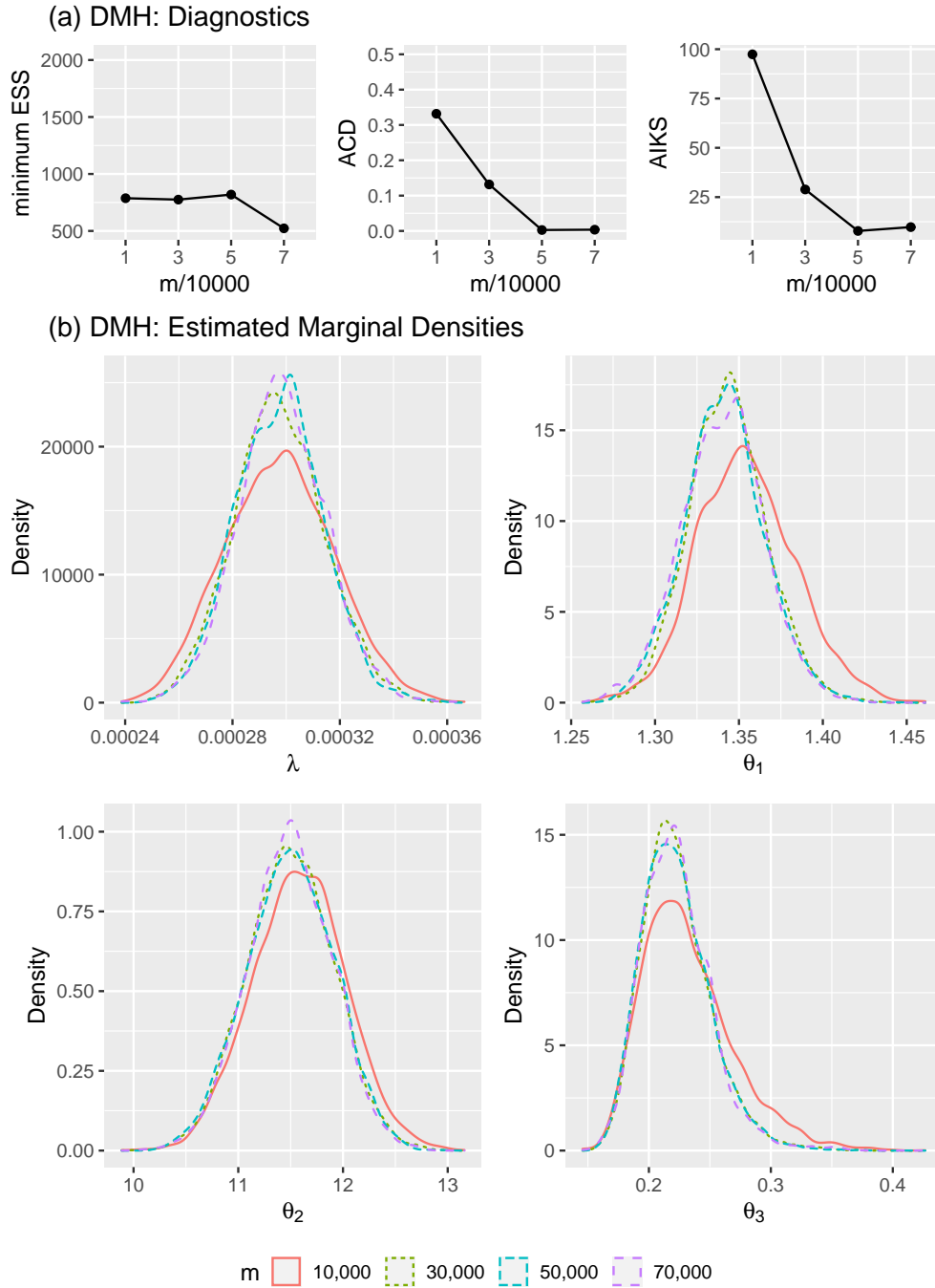


Figure 4: RSV point pattern from 1A2A-16h experiment. **(a)** Diagnostics (minimum ESS, ACD, AIKS) applied to samples generated from DMH with different numbers  $m$  of (inner) birth-death updates. A larger ESS is better, a smaller ACD is better, and a smaller AIKS is better. **(b)** Estimated marginal posterior densities of the samples. ACD and AIKS recommend  $m$  of at least 50,000, while the minimum ESS is similar for the different values of  $m$ .

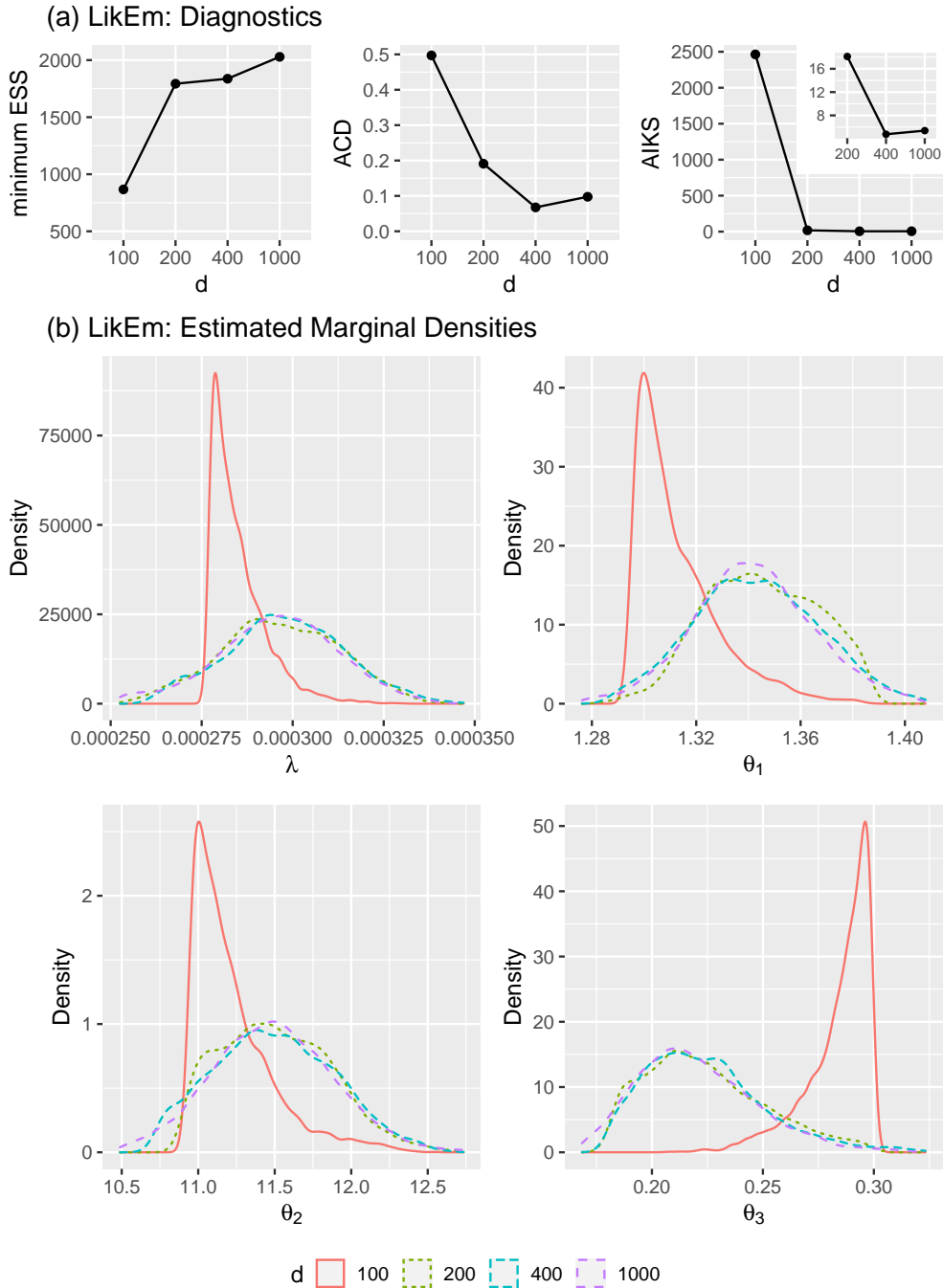


Figure 5: RSV point pattern from 1A2A-16h experiment. **(a)** Diagnostics (minimum ESS, ACD, AIKS) applied to samples generated from LikEm with different numbers  $d$  of particles. The subplot within the AIKS plot shows close-up of the right end of the plot. A larger ESS is better, a smaller ACD is better, and a smaller AIKS is better. **(b)** Estimated posterior marginal densities of the samples. Here the minimum ESS happens to provide similar conclusion to ACD and AIKS.

puting, we thinned the samples at equally spaced intervals of 10 to obtain 5,000 sample points. When calculating ACD and AIKS, two independent sets of  $N = 100,000$  auxiliary samples are generated from the likelihood via the birth-death sampler for approximating the score function,  $H$  matrix, and  $J$  matrix at each of the sample points. We used parallel computing to obtain the approximations and to compute AIKS. For a posterior sample path, the approximation step took at most 23.9 hours. Given the approximations, the longest ACD computation took 5.4 seconds and the longest AIKS computation took 11.1 seconds.

For DMH, Figure 4 (a) shows that the minimum ESS is pretty small at every choice of  $m$  (its maximum is 819 at  $m = 50,000$ ). ACD and AIKS have their largest values at  $m = 10,000$  and generally decrease (become better) as  $m$  increases. Both ACD and AIKS imply that  $m$  should be at least 50,000 (they are minimized at  $m = 50,000$  where ACD is 0.0026 and AIKS is 7.836). In Figure 4 (b), it is observed that the estimated marginal posterior densities of the sample with  $m = 10,000$  are different from the others. This shows agreement with the result that ACD and AIKS are the largest at  $m = 10,000$ . Figure 5 (a) shows the diagnostic values for the LikEm samples. All of them imply that the samples generally become better as  $d$  increases. The minimum ESS is maximized at  $d = 1,000$  (it is 2,029 at  $d = 1,000$ ). ACD and AIKS indicate that  $d$  should be at least 400 (both are minimized at  $d = 400$  where ACD is 0.068 and AIKS is 4.771). In Figure 5 (b), we observe that the estimated marginal posterior densities of the sample with  $d = 100$  are significantly different from the others. The minimum ESS has the smallest value for that sample. ACD and AIKS also have the largest values for that sample of all the examples in this article.

In this case, all the diagnostics agree.

## 7 Discussion

In this article we proposed new methods that provide guidance for tuning algorithms and give some measure of sample quality for a wide range of Monte Carlo algorithms, including a particularly challenging class of algorithms: asymptotically inexact algorithms for distributions with intractable normalising functions. We describe three methods. CD applies broadly to most any likelihood-based context where misspecification is of concern while ACD and AIKS are specifically targeted at likelihoods with intractable normalising functions. Our study mainly focuses on intractable normalising function problems and shows that our methods can assess the quality of samples and provide good guidance for tuning algorithms. We have studied applications of ACD and AIKS to several asymptotically exact and inexact algorithms in the context of challenging simulated and real data examples. This shows that our methods provide useful results not only for asymptotically exact algorithms, for which some other methods may be useful, but also for asymptotically inexact algorithms, for which no other methods exist.

We note that ACD and AIKS could be slightly different in their conclusions as our examples in Section 6 illustrate, but the difference is quite small and overall conclusions are pretty much the same. The difference between ACD and AIKS stems from the fact that they consider different sets of test functions to quantify the difference between a sample mean and a target expectation. ACD considers two functions whose target expectations are identical and measures the difference between sample means of the two functions. AIKS

considers a set of functions whose target expectations are zero and finds the maximum error between the sample mean and the target expectation. Unless the score function of the target density is the origin, their sets of test functions are mutually exclusive, which is the case of all the examples in this article. Depending on the setting, ACD or AIKS may be more useful. ACD has a restricted range between 0 and 1 and thus its result is more easily interpretable compared to AIKS whose scale varies from problem to problem. However, one advantage of AIKS is that it is supported by a theory of weak convergence and thus can be used for deciding convergence of a sequence of sample points to the target distribution.

ACD and AIKS are obtained by replacing some functions that have to be evaluated for CD and IMQ KSD with their Monte Carlo approximations. This allows for the diagnostics to be available for doubly intractable posterior distributions. However, an open question is how many Monte Carlo samples  $N$  to use for the approximation. In this article we choose  $N = 100,000$  based on a simulation study where CD and IMQ KSD are attainable so that we can compare the approximate versions with the exact versions of the diagnostics. The computing time of ACD and AIKS mainly accounts for the Monte Carlo approximation, which might be computationally expensive for high-dimensional datasets. However, the approximation step is embarrassingly parallel in that the Monte Carlo estimates at the posterior sample points can be constructed entirely in parallel. Therefore, the computational expense can be decreased by a factor corresponding to the number of available cores. This can be helpful provided that the availability of parallel computing resources increases. We note that a good outcome of ACD for a sample, that is, ACD close to 0, is a necessary

but not a sufficient condition to trust that the asymptotic distribution of the sample is close to the target distribution. Furthermore, careful approaches for deciding thresholds for ACD and AIKS is still an open problem. Developing theoretical support for ACD and a way of deciding the thresholds may provide interesting avenues for future research.

## Acknowledgements

The authors are grateful to Jaewoo Park for providing useful code and to Galin Jones for helpful comments. JH and MH were partially supported by the National Institute of General Medical Sciences of the National Institutes of Health under Award Number R01GM123007

## References

- Alquier, P., Friel, N., Everitt, R., and Boland, A. (2016). Noisy Monte Carlo: Convergence of Markov chains with approximate transition kernels. *Statistics and Computing*, 26(1-2):29–47.
- Atchadé, Y. F., Lartillot, N., and Robert, C. (2013). Bayesian computation for statistical models with intractable normalizing constants. *Brazilian Journal of Probability and Statistics*, 27(4):416–436.
- Bartlett, M. S. (1953a). Approximate confidence intervals. *Biometrika*, 40(1/2):12–19.

- Bartlett, M. S. (1953b). Approximate confidence intervals. II. More than one unknown parameter. *Biometrika*, 40(3/4):306–317.
- Besag, J. (1974). Spatial interaction and the statistical analysis of lattice systems. *Journal of the Royal Statistical Society: Series B*, 36(2):192–225.
- Cowles, M. K. and Carlin, B. P. (1996). Markov chain Monte Carlo convergence diagnostics: A comparative review. *Journal of the American Statistical Association*, 91(434):883–904.
- Eddelbuettel, D. and Francois, R. (2011). Rcpp: Seamless R and C++ integration. *Journal of Statistical Software*, 40:1–18.
- Fan, Y., Brooks, S. P., and Gelman, A. (2006). Output assessment for Monte Carlo simulations via the score statistic. *Journal of Computational and Graphical Statistics*, 15(1):178–206.
- Flegal, J. M. and Jones, G. L. (2011). Implementing MCMC: Estimating with confidence. In *Handbook of Markov Chain Monte Carlo*, chapter 7, pages 175–197. CRC Press.
- Goldstein, J., Haran, M., Simeonov, I., Fricks, J., and Chiaromonte, F. (2015). An attraction-repulsion point process model for respiratory syncytial virus infections. *Biometrics*, 71(2):376–385.
- Gorham, J. and Mackey, L. (2015). Measuring sample quality with Stein’s method. In *Advances in Neural Information Processing Systems*, volume 28, pages 226–234.
- Gorham, J. and Mackey, L. (2017). Measuring sample quality with kernels. In *Proceedings*

- of the 34th International Conference on Machine Learning, volume 70 of *Proceedings of Machine Learning Research*, pages 1292–1301.
- Hastings, W. K. (1970). Monte Carlo sampling methods using Markov chains and their applications. *Biometrika*, 57(1):97–109.
- Hughes, J., Haran, M., and Caragea, P. C. (2011). Autologistic models for binary data on a lattice. *Environmetrics*, 22(7):857–871.
- Hunter, D. R. (2007). Curved exponential family models for social networks. *Social Networks*, 29(2):216–230.
- Hunter, D. R. and Handcock, M. S. (2006). Inference in curved exponential family models for networks. *Journal of Computational and Graphical Statistics*, 15(3):565–583.
- Hunter, D. R., Handcock, M. S., Butts, C. T., Goodreau, S. M., and Morris, M. (2008). ergm: A package to fit, simulate and diagnose exponential-family models for networks. *Journal of Statistical Software*, 24(3):1–29.
- Ihaka, R. and Gentleman, R. (1996). R: A language for data analysis and graphics. *Journal of Computational and Graphical Statistics*, 5(3):299–314.
- Ising, E. (1925). Beitrag zur theorie des ferromagnetismus. *Zeitschrift für Physik A Hadrons and Nuclei*, 31(1):253–258.
- Kass, R. E., Carlin, B. P., Gelman, A., and Neal, R. M. (1998). Markov Chain Monte Carlo in Practice: A Roundtable Discussion. *The American Statistician*, 52(2):93–100.

- Lee, J. E., Nicholls, G. K., and Ryder, R. J. (2019). Calibration Procedures for Approximate Bayesian Credible Sets. *Bayesian Analysis*, 14(4):1245–1269.
- Lenz, W. (1920). Beitrag zum Verständnis der magnetischen Erscheinungen in festen Körpern. *Physikalische Zeitschrift*, 21:613–615.
- Liang, F. (2010). A double Metropolis-Hastings sampler for spatial models with intractable normalizing constants. *Journal of Statistical Computation and Simulation*, 80(9):1007–1022.
- Liang, F., Jin, I. H., Song, Q., and Liu, J. S. (2016). An adaptive exchange algorithm for sampling from distributions with intractable normalizing constants. *Journal of the American Statistical Association*, 111(513):377–393.
- Lyne, A. M., Girolami, M., Atchadé, Y., Strathmann, H., and Simpson, D. (2015). On Russian Roulette estimates for Bayesian inference with doubly-intractable likelihoods. *Statistical Science*, 30(4):443–467.
- Metropolis, N., Rosenbluth, A. W., Rosenbluth, M. N., Teller, A. H., and Teller, E. (1953). Equation of state calculations by fast computing machines. *The journal of chemical physics*, 21(6):1087–1092.
- Møller, J., Pettitt, A. N., Reeves, R., and Berthelsen, K. K. (2006). An efficient Markov chain Monte Carlo method for distributions with intractable normalising constants. *Biometrika*, 93(2):451–458.

- Müller, A. (1997). Integral probability metrics and their generating classes of functions. *Advances in Applied Probability*, 29(2):429–443.
- Murray, I., Ghahramani, Z., and Mackay, D. J. C. (2006). MCMC for doubly-intractable distributions. In *Proceedings of the 22nd Annual Conference on Uncertainty in Artificial Intelligence*, pages 359–366.
- Park, J. and Haran, M. (2018). Bayesian inference in the presence of intractable normalizing functions. *Journal of the American Statistical Association*, 113(523):1372–1390.
- Park, J. and Haran, M. (2020). A function emulation approach for doubly intractable distributions. *Journal of Computational and Graphical Statistics*, 29(1):66–77.
- Propp, J. G. and Wilson, D. B. (1996). Exact sampling with coupled Markov chains and applications to statistical mechanics. *Random Structures & Algorithms*, 9(1-2):223–252.
- Robert, C. and Casella, G. (2013). *Monte Carlo statistical methods*. Springer Science & Business Media, New York.
- Robins, G., Pattison, P., Kalish, Y., and Lusher, D. (2007). An introduction to exponential random graph ( $p^*$ ) models for social networks. *Social Networks*, 29(2):173–191.
- Roy, V. (2020). Convergence diagnostics for Markov chain Monte Carlo. *Annual Review of Statistics and Its Application*, 7:387–412.
- Stein, C. (1972). A bound for the error in the normal approximation to the distribution of a sum of dependent random variables. In *Proceedings of the Sixth Berkeley Symposium on Mathematical Statistics and Probability*, volume 2, pages 583–602.

Strauss, D. J. (1975). A model for clustering. *Biometrika*, 62(2):467–475.

Xing, H., Nicholls, G. K., and Lee, J. E. (2019). Calibrated approximate Bayesian inference.

In *Proceedings of the 36th International Conference on Machine Learning*, volume 97 of *Proceedings of Machine Learning Research*, pages 6912–6920.

# Supplementary Material for Diagnostics for Monte Carlo Algorithms for Models with Intractable normalising Functions

Bokgyeong Kang, John Hughes, and Murali Haran

December 3, 2021

## A A toy example

Here we use a toy example to choose the auxiliary sample size  $N$  such that ACD and AIKS are reliable approximations to CD and IMQ KSD, respectively. For a univariate Gaussian model, we compute all diagnostics and compare the exact versions with the approximate versions, i.e., we compare CD with ACD, and IMQ KSD with AIKS.

Observations  $x_1, \dots, x_n$  are generated independently and identically from the  $N(\mu, \sigma^2)$  distribution. The prior distributions for the parameters are  $\mu \sim N(0, 100)$  and  $\sigma^2 \sim \text{IG}(0.001, 0.001)$ . A posterior sample path is generated via Gibbs sampling. For the posterior sample path, CD and IMQ KSD are computed. We assume that the normalising function of the likelihood is intractable and compute ACD and AIKS, where we generate two independent sets of  $N = 100,000$  auxiliary variables via the Metropolis–Hastings algorithm to approximate the score function, the Hessian matrix, and the outer product of the score function of the posterior density.

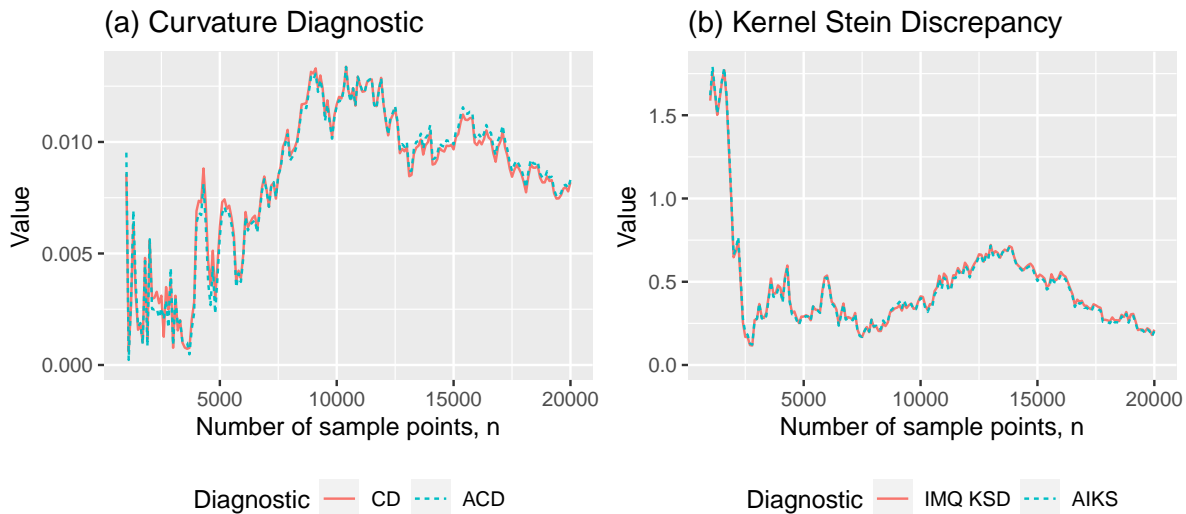


Figure 1: (a) CD and ACD for the posterior sample generated via Gibbs sampler in the univariate Gaussian example. (b) IMQ KSD and AIKS for the same posterior sample.

In Figure 1 (a), CD and ACD are plotted as functions of the first  $n$  sample points. This shows that ACD almost perfectly approximates CD over the entire sample path. We plot IMQ KSD and AIKS as functions of the first  $n$  sample points in Figure 1 (b), from which we see that AIKS also closely approximates IMQ KSD for  $N = 100,000$ . Table 1 shows values of all the diagnostics for the first  $n$  sample points where  $n = 5,000, 10,000, 15,000,$  and  $20,000$ . We see that the approximations are quite close to the true values.

In summary, this example shows that ACD and AIKS provide reliable approximations to CD and IMQ KSD, respectively, for  $N = 100,000$ .

Number of sample points, $n$	CD	ACD	IMQ KSD	AIKS
5,000	0.0062	0.0058	0.2908	0.2822
10,000	0.0117	0.0116	0.4124	0.4021
15,000	0.0097	0.0099	0.5216	0.5048
20,000	0.0082	0.0083	0.2122	0.2030

Table 1: Comparison of CD with ACD, and comparison of IMQ KSD with AIKS, in the univariate Gaussian example.

## B Proof of Theorem 1

### B.1 Score function of normalising function

For a  $p$ -dimensional parameter vector  $\boldsymbol{\theta}$ , consider a posterior density  $\pi(\boldsymbol{\theta} \mid \boldsymbol{x})$  whose likelihood function is  $L(\boldsymbol{\theta} \mid \boldsymbol{x}) = h(\boldsymbol{x} \mid \boldsymbol{\theta})/c(\boldsymbol{\theta})$  and prior density is  $p(\boldsymbol{\theta})$ . The  $k$ th element of the score function of the normalising function  $c(\boldsymbol{\theta})$  can be written as

$$\begin{aligned}
 \frac{\partial \log c(\boldsymbol{\theta})}{\partial \theta_k} &= \frac{1}{c(\boldsymbol{\theta})} \frac{\partial c(\boldsymbol{\theta})}{\partial \theta_k} \\
 &= \frac{1}{c(\boldsymbol{\theta})} \frac{\partial}{\partial \theta_k} \int_{\boldsymbol{x}} h(\boldsymbol{x} \mid \boldsymbol{\theta}) d\boldsymbol{x} \\
 &= \frac{1}{c(\boldsymbol{\theta})} \int_{\boldsymbol{x}} \frac{\partial h(\boldsymbol{x} \mid \boldsymbol{\theta})}{\partial \theta_k} d\boldsymbol{x} \tag{1} \\
 &= \frac{1}{c(\boldsymbol{\theta})} \int_{\boldsymbol{x}} h(\boldsymbol{x} \mid \boldsymbol{\theta}) \frac{\partial \log h(\boldsymbol{x} \mid \boldsymbol{\theta})}{\partial \theta_k} d\boldsymbol{x} \\
 &= \int_{\boldsymbol{x}} \frac{\partial \log h(\boldsymbol{x} \mid \boldsymbol{\theta})}{\partial \theta_k} f(\boldsymbol{x} \mid \boldsymbol{\theta}) d\boldsymbol{x} \\
 &= \mathbb{E}_f \left\{ \frac{\partial \log h(\boldsymbol{X} \mid \boldsymbol{\theta})}{\partial \theta_k} \right\}. \tag{2}
 \end{aligned}$$

Equation (1) follows from the dominated convergence theorem. Under the assumptions that the score function exists and the score function and the normalising function are bounded, we have exchanged the derivative with the integral.

### B.2 Hessian matrix of normalising function

The  $(k, l)$ th entry of the Hessian matrix of the normalising function  $c(\boldsymbol{\theta})$  is given by

$$\begin{aligned}
 \frac{\partial^2 \log c(\boldsymbol{\theta})}{\partial \theta_k \partial \theta_l} &= \frac{\partial}{\partial \theta_k} \left\{ \frac{1}{c(\boldsymbol{\theta})} \frac{\partial c(\boldsymbol{\theta})}{\partial \theta_l} \right\} \\
 &= \frac{1}{c(\boldsymbol{\theta})} \frac{\partial^2 c(\boldsymbol{\theta})}{\partial \theta_k \partial \theta_l} - \left\{ \frac{1}{c(\boldsymbol{\theta})} \frac{\partial c(\boldsymbol{\theta})}{\partial \theta_k} \right\} \left\{ \frac{1}{c(\boldsymbol{\theta})} \frac{\partial c(\boldsymbol{\theta})}{\partial \theta_l} \right\} \\
 &= \frac{1}{c(\boldsymbol{\theta})} \frac{\partial^2 c(\boldsymbol{\theta})}{\partial \theta_k \partial \theta_l} - \mathbb{E}_f \left\{ \frac{\partial \log h(\boldsymbol{X} \mid \boldsymbol{\theta})}{\partial \theta_k} \right\} \mathbb{E}_f \left\{ \frac{\partial \log h(\boldsymbol{X} \mid \boldsymbol{\theta})}{\partial \theta_l} \right\}. \tag{3}
 \end{aligned}$$

Now consider the first term on the right hand side of equation (3). It can be written as

$$\begin{aligned} \frac{1}{c(\boldsymbol{\theta})} \frac{\partial^2 c(\boldsymbol{\theta})}{\partial \theta_k \partial \theta_l} &= \frac{1}{c(\boldsymbol{\theta})} \frac{\partial^2}{\partial \theta_k \partial \theta_l} \int_{\mathbf{x}} h(\mathbf{x}|\boldsymbol{\theta}) d\mathbf{x} \\ &= \frac{1}{c(\boldsymbol{\theta})} \int_{\mathbf{x}} \frac{\partial}{\partial \theta_k} \left\{ \frac{\partial \log h(\mathbf{x}|\boldsymbol{\theta})}{\partial \theta_l} h(\mathbf{x}|\boldsymbol{\theta}) \right\} d\mathbf{x} \end{aligned} \quad (4)$$

$$\begin{aligned} &= \int_{\mathbf{x}} \frac{\partial^2 \log h(\mathbf{x}|\boldsymbol{\theta})}{\partial \theta_k \partial \theta_l} f(\mathbf{x}|\boldsymbol{\theta}) d\mathbf{x} + \int_{\mathbf{x}} \frac{\partial \log h(\mathbf{x}|\boldsymbol{\theta})}{\partial \theta_k} \frac{\partial \log h(\mathbf{x}|\boldsymbol{\theta})}{\partial \theta_l} f(\mathbf{x}|\boldsymbol{\theta}) d\mathbf{x} \\ &= \mathbb{E}_f \left\{ \frac{\partial^2 \log h(\mathbf{X}|\boldsymbol{\theta})}{\partial \theta_k \partial \theta_l} \right\} + \mathbb{E}_f \left\{ \frac{\partial \log h(\mathbf{X}|\boldsymbol{\theta})}{\partial \theta_k} \frac{\partial \log h(\mathbf{X}|\boldsymbol{\theta})}{\partial \theta_l} \right\}. \end{aligned} \quad (5)$$

In the equation (4) we have exchanged the derivative with the integral, owing to the dominated convergence theorem. Combining (3) and (5), the  $(k, l)$ th entry of the Hessian matrix of the normalising function  $c(\boldsymbol{\theta})$  is

$$\begin{aligned} \frac{\partial^2 \log c(\boldsymbol{\theta})}{\partial \theta_k \partial \theta_l} &= \mathbb{E}_f \left\{ \frac{\partial^2 \log h(\mathbf{X}|\boldsymbol{\theta})}{\partial \theta_k \partial \theta_l} \right\} + \mathbb{E}_f \left\{ \frac{\partial \log h(\mathbf{X}|\boldsymbol{\theta})}{\partial \theta_k} \frac{\partial \log h(\mathbf{X}|\boldsymbol{\theta})}{\partial \theta_l} \right\} \\ &\quad - \mathbb{E}_f \left\{ \frac{\partial \log h(\mathbf{X}|\boldsymbol{\theta})}{\partial \theta_k} \right\} \mathbb{E}_f \left\{ \frac{\partial \log h(\mathbf{X}|\boldsymbol{\theta})}{\partial \theta_l} \right\}. \end{aligned}$$

### B.3 Approximation error of sensitivity matrix

Suppose  $\boldsymbol{\theta}^{(1)}, \dots, \boldsymbol{\theta}^{(n)}$  is a sequence of sample points whose asymptotic distribution is equal to the posterior distribution  $\pi(\boldsymbol{\theta} | \mathbf{x})$ . Let  $H(\boldsymbol{\theta})$  be the Hessian matrix of the posterior density function. The Hessian's unbiased Monte Carlo estimate  $\hat{H}(\boldsymbol{\theta})$  can be obtained as follows. The  $(k, l)$ th entry of  $\hat{H}(\boldsymbol{\theta})$  is

$$\begin{aligned} \hat{H}_{k,l}(\boldsymbol{\theta}) &= \frac{\partial^2 \log p(\boldsymbol{\theta})}{\partial \theta_k \partial \theta_l} + \frac{\partial^2 \log h(\mathbf{x}|\boldsymbol{\theta})}{\partial \theta_k \partial \theta_l} - \frac{1}{2N} \sum_{j=1}^{2N} \frac{\partial^2 \log h(\mathbf{y}^{(j)}|\boldsymbol{\theta})}{\partial \theta_k \partial \theta_l} \\ &\quad - \frac{1}{2N} \sum_{j=1}^{2N} \left\{ \frac{\partial \log h(\mathbf{y}^{(j)}|\boldsymbol{\theta})}{\partial \theta_k} \right\} \left\{ \frac{\partial \log h(\mathbf{y}^{(j)}|\boldsymbol{\theta})}{\partial \theta_l} \right\} \\ &\quad + \left\{ \frac{1}{N} \sum_{j=1}^N \frac{\partial \log h(\mathbf{y}^{(j)}|\boldsymbol{\theta})}{\partial \theta_k} \right\} \left\{ \frac{1}{N} \sum_{j=N+1}^{2N} \frac{\partial \log h(\mathbf{y}^{(j)}|\boldsymbol{\theta})}{\partial \theta_l} \right\}, \end{aligned}$$

where  $\mathbf{y}^{(1)}, \dots, \mathbf{y}^{(N)}$  and  $\mathbf{y}^{(N+1)}, \dots, \mathbf{y}^{(2N)}$  are two independent sets of auxiliary variables generated from  $f(\cdot | \boldsymbol{\theta})$ .

Let  $\mathcal{H}(\mathbf{x}) = \mathbb{E}_\pi \{-H(\boldsymbol{\theta})\}$  be the sensitivity matrix of the posterior density function and  $\hat{\mathcal{H}}(\mathbf{x}) = \frac{1}{n} \sum_{i=1}^n -\hat{H}(\boldsymbol{\theta}^{(i)})$  be its two-stage approximation. For every  $k, l \in \{1, \dots, p\}$ , the

difference between their  $(k, l)$ th entries is

$$\begin{aligned}
\left| \mathcal{H}_{k,l}(\mathbf{x}) - \hat{\mathcal{H}}_{k,l}(\mathbf{x}) \right| &= \left| \frac{1}{n} \sum_{i=1}^n \hat{H}_{k,l}(\boldsymbol{\theta}^{(i)}) - \mathbb{E}_\pi \{ H_{k,l}(\boldsymbol{\theta}) \} \right| \\
&\leq \left| \frac{1}{n} \sum_{i=1}^n H_{k,l}(\boldsymbol{\theta}^{(i)}) - \mathbb{E}_\pi \{ H_{k,l}(\boldsymbol{\theta}) \} \right| + \left| \frac{1}{n} \sum_{i=1}^n \left\{ \hat{H}_{k,l}(\boldsymbol{\theta}^{(i)}) - H_{k,l}(\boldsymbol{\theta}^{(i)}) \right\} \right| \\
&\leq \delta_1(n) + \frac{1}{n} \sum_{i=1}^n \left| \hat{H}_{k,l}(\boldsymbol{\theta}^{(i)}) - H_{k,l}(\boldsymbol{\theta}^{(i)}) \right|, \tag{6}
\end{aligned}$$

where  $\delta_1(n) = \left\| \frac{1}{n} \sum_{i=1}^n H(\boldsymbol{\theta}^{(i)}) - \mathbb{E}_\pi \{ H(\boldsymbol{\theta}) \} \right\|_\infty$  and  $\delta_1(n)$  goes to 0 as  $n$  increases. The inequality (6) follows from the ergodic theorem. Thus the Monte Carlo estimates converge to the truth almost surely. Now we consider the second term on the right hand side of inequality (6). Let

$$\begin{aligned}
\epsilon_1(N) &= \max_{k,l} \left| \frac{1}{2N} \sum_{j=1}^{2N} \frac{\partial^2 \log h(\mathbf{y}^{(j)}|\boldsymbol{\theta})}{\partial \theta_k \partial \theta_l} - \mathbb{E}_f \left\{ \frac{\partial^2 \log h(\mathbf{X}|\boldsymbol{\theta})}{\partial \theta_k \partial \theta_l} \right\} \right|, \\
\epsilon_2(N) &= \max_{k,l} \left| \frac{1}{2N} \sum_{j=1}^{2N} \left\{ \frac{\partial \log h(\mathbf{y}^{(j)}|\boldsymbol{\theta})}{\partial \theta_k} \right\} \left\{ \frac{\partial \log h(\mathbf{y}^{(j)}|\boldsymbol{\theta})}{\partial \theta_l} \right\} - \mathbb{E}_f \left\{ \frac{\partial \log h(\mathbf{X}|\boldsymbol{\theta})}{\partial \theta_k} \frac{\partial \log h(\mathbf{X}|\boldsymbol{\theta})}{\partial \theta_l} \right\} \right|, \\
\epsilon_3(N) &= \max_k \left| \frac{1}{N} \sum_{j=1}^N \frac{\partial \log h(\mathbf{y}^{(j)}|\boldsymbol{\theta})}{\partial \theta_k} - \mathbb{E}_f \left\{ \frac{\partial \log h(\mathbf{X}|\boldsymbol{\theta})}{\partial \theta_k} \right\} \right|, \\
\epsilon_4(N) &= \max_l \left| \frac{1}{N} \sum_{j=N+1}^{2N} \frac{\partial \log h(\mathbf{y}^{(j)}|\boldsymbol{\theta})}{\partial \theta_l} - \mathbb{E}_f \left\{ \frac{\partial \log h(\mathbf{X}|\boldsymbol{\theta})}{\partial \theta_l} \right\} \right|,
\end{aligned}$$

and  $\epsilon(N) = \max \{ \epsilon_1(N), \epsilon_2(N), \epsilon_3(N), \epsilon_4(N) \}$ . By the ergodic theorem,  $\epsilon(N)$  goes to 0 as  $N$  increases. Then we can bound the difference between  $\hat{H}(\boldsymbol{\theta})$  and  $H(\boldsymbol{\theta})$  as follows. For all

$k, l \in \{1, \dots, p\}$ , we have

$$\begin{aligned}
& \left| \hat{H}_{k,l}(\boldsymbol{\theta}) - H_{k,l}(\boldsymbol{\theta}) \right| \\
& \leq \left| \frac{1}{2N} \sum_{j=1}^{2N} \frac{\partial^2 \log h(\mathbf{y}^{(j)}|\boldsymbol{\theta})}{\partial \theta_k \partial \theta_l} - \mathbb{E}_f \left\{ \frac{\partial^2 \log h(\mathbf{X}|\boldsymbol{\theta})}{\partial \theta_k \partial \theta_l} \right\} \right| \\
& + \left| \frac{1}{2N} \sum_{j=1}^{2N} \left\{ \frac{\partial \log h(\mathbf{y}^{(j)}|\boldsymbol{\theta})}{\partial \theta_k} \right\} \left\{ \frac{\partial \log h(\mathbf{y}^{(j)}|\boldsymbol{\theta})}{\partial \theta_l} \right\} - \mathbb{E}_f \left\{ \frac{\partial \log h(\mathbf{X}|\boldsymbol{\theta})}{\partial \theta_k} \frac{\partial \log h(\mathbf{X}|\boldsymbol{\theta})}{\partial \theta_l} \right\} \right| \\
& + \left| \left\{ \frac{1}{N} \sum_{j=1}^N \frac{\partial \log h(\mathbf{y}^{(j)}|\boldsymbol{\theta})}{\partial \theta_k} \right\} \left\{ \frac{1}{N} \sum_{j=N+1}^{2N} \frac{\partial \log h(\mathbf{y}^{(j)}|\boldsymbol{\theta})}{\partial \theta_l} \right\} - \mathbb{E}_f \left\{ \frac{\partial \log h(\mathbf{X}|\boldsymbol{\theta})}{\partial \theta_k} \right\} \mathbb{E}_f \left\{ \frac{\partial \log h(\mathbf{X}|\boldsymbol{\theta})}{\partial \theta_l} \right\} \right| \\
& \leq 2\epsilon(N) + \left| \frac{1}{N} \sum_{j=1}^N \frac{\partial \log h(\mathbf{y}^{(j)}|\boldsymbol{\theta})}{\partial \theta_k} - \mathbb{E}_f \left\{ \frac{\partial \log h(\mathbf{X}|\boldsymbol{\theta})}{\partial \theta_k} \right\} \right| \left| \mathbb{E}_f \left\{ \frac{\partial \log h(\mathbf{X}|\boldsymbol{\theta})}{\partial \theta_l} \right\} \right| \\
& + \left| \frac{1}{N} \sum_{j=N+1}^{2N} \frac{\partial \log h(\mathbf{y}^{(j)}|\boldsymbol{\theta})}{\partial \theta_l} - \mathbb{E}_f \left\{ \frac{\partial \log h(\mathbf{X}|\boldsymbol{\theta})}{\partial \theta_l} \right\} \right| \left| \frac{1}{N} \sum_{j=1}^N \frac{\partial \log h(\mathbf{y}^{(j)}|\boldsymbol{\theta})}{\partial \theta_k} \right| \tag{7} \\
& \leq 2\epsilon(N) + \epsilon(N) \mathbb{E}_f \left| \frac{\partial \log h(\mathbf{X}|\boldsymbol{\theta})}{\partial \theta_l} \right| + \epsilon(N) \max_{j \in \{1, \dots, N\}} \left| \frac{\partial \log h(\mathbf{y}^{(j)}|\boldsymbol{\theta})}{\partial \theta_k} \right| \\
& \leq 2(1 + c_h)\epsilon(N). \tag{8}
\end{aligned}$$

Inequality (7) follows from the following elementary inequality.

$$|ab - \hat{a}\hat{b}| = |ab - \hat{a}b + \hat{a}b - \hat{a}\hat{b}| = |(a - \hat{a})b + (b - \hat{b})\hat{a}| \leq |a - \hat{a}||b| + |b - \hat{b}||\hat{a}| \tag{9}$$

Inequality (8) is from Assumption 2 in Theorem 1. Therefore, the approximation error for the sensitivity matrix is

$$\|\mathcal{H}(\mathbf{x}) - \hat{\mathcal{H}}(\mathbf{x})\|_\infty \leq \delta_1(n) + 2(1 + c_h)\epsilon(N) \tag{10}$$

almost surely.

## B.4 Approximation error of variability matrix

Let  $J(\boldsymbol{\theta})$  be the outer product of the score function of the posterior density function.  $J(\boldsymbol{\theta})$ 's unbiased Monte Carlo estimate  $\hat{J}(\boldsymbol{\theta})$  can be obtained as follows. The  $(k, l)$ th entry of  $\hat{J}(\boldsymbol{\theta})$

is

$$\begin{aligned}
\hat{J}_{k,l}(\boldsymbol{\theta}) &= \left\{ \frac{\partial \log p(\boldsymbol{\theta})}{\partial \theta_k} + \frac{\partial \log h(\mathbf{x}|\boldsymbol{\theta})}{\partial \theta_k} \right\} \left\{ \frac{\partial \log p(\boldsymbol{\theta})}{\partial \theta_l} + \frac{\partial \log h(\mathbf{x}|\boldsymbol{\theta})}{\partial \theta_l} \right\} \\
&+ \left\{ \frac{\partial \log p(\boldsymbol{\theta})}{\partial \theta_k} + \frac{\partial \log h(\mathbf{x}|\boldsymbol{\theta})}{\partial \theta_k} \right\} \left\{ \frac{1}{N} \sum_{j=N+1}^{2N} \frac{\partial \log h(\mathbf{y}^{(j)}|\boldsymbol{\theta})}{\partial \theta_l} \right\} \\
&+ \left\{ \frac{\partial \log p(\boldsymbol{\theta})}{\partial \theta_l} + \frac{\partial \log h(\mathbf{x}|\boldsymbol{\theta})}{\partial \theta_l} \right\} \left\{ \frac{1}{N} \sum_{j=1}^N \frac{\partial \log h(\mathbf{y}^{(j)}|\boldsymbol{\theta})}{\partial \theta_k} \right\} \\
&+ \left\{ \frac{1}{N} \sum_{j=1}^N \frac{\partial \log h(\mathbf{y}^{(j)}|\boldsymbol{\theta})}{\partial \theta_k} \right\} \left\{ \frac{1}{N} \sum_{j=N+1}^{2N} \frac{\partial \log h(\mathbf{y}^{(j)}|\boldsymbol{\theta})}{\partial \theta_l} \right\},
\end{aligned}$$

where  $\mathbf{y}^{(1)}, \dots, \mathbf{y}^{(N)}$  and  $\mathbf{y}^{(N+1)}, \dots, \mathbf{y}^{(2N)}$  are two independent sets of auxiliary variables generated from  $f(\cdot | \boldsymbol{\theta})$ .

Let  $\mathcal{J}(\mathbf{x}) = \mathbb{E}_\pi\{J(\boldsymbol{\theta})\}$  be the variability matrix of the posterior density function and  $\hat{\mathcal{J}}(\mathbf{x}) = \frac{1}{n} \sum_{i=1}^n \hat{J}(\boldsymbol{\theta}^{(i)})$  be its two-stage approximation. For all  $k, l \in \{1, \dots, p\}$ , the difference between the matrices'  $(k, l)$ th entries is

$$\begin{aligned}
\left| \mathcal{J}_{k,l}(\mathbf{x}) - \hat{\mathcal{J}}_{k,l}(\mathbf{x}) \right| &= \left| \frac{1}{n} \sum_{i=1}^n \hat{J}_{k,l}(\boldsymbol{\theta}^{(i)}) - \mathbb{E}_\pi\{J_{k,l}(\boldsymbol{\theta})\} \right| \\
&\leq \left| \frac{1}{n} \sum_{i=1}^n J_{k,l}(\boldsymbol{\theta}^{(i)}) - \mathbb{E}_\pi\{J_{k,l}(\boldsymbol{\theta})\} \right| + \left| \frac{1}{n} \sum_{i=1}^n \left\{ \hat{J}_{k,l}(\boldsymbol{\theta}^{(i)}) - J_{k,l}(\boldsymbol{\theta}^{(i)}) \right\} \right| \\
&\leq \delta_2(n) + \frac{1}{n} \sum_{i=1}^n \left| \hat{J}_{k,l}(\boldsymbol{\theta}^{(i)}) - J_{k,l}(\boldsymbol{\theta}^{(i)}) \right|, \tag{11}
\end{aligned}$$

where  $\delta_2(n) = \left\| \frac{1}{n} \sum_{i=1}^n J(\boldsymbol{\theta}^{(i)}) - \mathbb{E}_\pi\{J(\boldsymbol{\theta})\} \right\|_\infty$  and  $\delta_2(n)$  goes to 0 as  $n$  increases. Inequality (11) is from the ergodic theorem. This implies that the Monte Carlo estimates converge to the truth almost surely. Now we consider the second term on the right hand side of inequality (11). We can bound the difference between  $\hat{J}(\boldsymbol{\theta})$  and  $J(\boldsymbol{\theta})$  as follows. For all

$k, l \in \{1, \dots, p\}$ , we have

$$\begin{aligned}
& \left| \hat{J}_{k,l}(\boldsymbol{\theta}) - J_{k,l}(\boldsymbol{\theta}) \right| \\
& \leq \left| \frac{\partial \log p(\boldsymbol{\theta})}{\partial \theta_k} + \frac{\partial \log h(\mathbf{x}|\boldsymbol{\theta})}{\partial \theta_k} \right| \left| \frac{1}{N} \sum_{j=N+1}^{2N} \frac{\partial \log h(\mathbf{y}^{(j)}|\boldsymbol{\theta})}{\partial \theta_l} - \mathbb{E}_f \left\{ \frac{\partial \log h(\mathbf{X}|\boldsymbol{\theta})}{\partial \theta_l} \right\} \right| \\
& + \left| \frac{\partial \log p(\boldsymbol{\theta})}{\partial \theta_l} + \frac{\partial \log h(\mathbf{x}|\boldsymbol{\theta})}{\partial \theta_l} \right| \left| \frac{1}{N} \sum_{j=1}^N \frac{\partial \log h(\mathbf{y}^{(j)}|\boldsymbol{\theta})}{\partial \theta_k} - \mathbb{E}_f \left\{ \frac{\partial \log h(\mathbf{X}|\boldsymbol{\theta})}{\partial \theta_k} \right\} \right| \\
& + \left| \left\{ \frac{1}{N} \sum_{j=1}^N \frac{\partial \log h(\mathbf{y}^{(j)}|\boldsymbol{\theta})}{\partial \theta_k} \right\} \left\{ \frac{1}{N} \sum_{j=N+1}^{2N} \frac{\partial \log h(\mathbf{y}^{(j)}|\boldsymbol{\theta})}{\partial \theta_l} \right\} - \mathbb{E}_f \left\{ \frac{\partial \log h(\mathbf{X}|\boldsymbol{\theta})}{\partial \theta_k} \right\} \mathbb{E}_f \left\{ \frac{\partial \log h(\mathbf{X}|\boldsymbol{\theta})}{\partial \theta_l} \right\} \right| \\
& \leq 2(2c_h + c_p)\epsilon(N). \tag{12}
\end{aligned}$$

Note that (12) is from (9) and Assumption 1–2 in Theorem 1. Therefore, the approximation error for the variability matrix is

$$\|\mathcal{J}(\mathbf{x}) - \hat{\mathcal{J}}(\mathbf{x})\|_\infty \leq \delta_2(n) + 2(2c_h + c_p)\epsilon(N) \tag{13}$$

almost surely.

## C Proof of Theorem 2

Consider a target distribution  $P$  and a weighted sample  $Q_n = \sum_{i=1}^n q_n(\boldsymbol{\theta}^{(i)})\delta_{\boldsymbol{\theta}^{(i)}}$  targeting  $P$ , where  $\boldsymbol{\theta}^{(1)}, \dots, \boldsymbol{\theta}^{(n)}$  are sample points and  $q_n$  is a probability mass function. By Minkowski's inequality, the difference between IMQ KSD and AIKS of  $Q_n$  is

$$\left| \hat{\mathcal{S}}(Q_n, \mathcal{T}_P, \mathcal{G}_{k, \|\cdot\|_p}) - \mathcal{S}(Q_n, \mathcal{T}_P, \mathcal{G}_{k, \|\cdot\|_p}) \right| \leq \|\hat{\mathbf{w}} - \mathbf{w}\|_p.$$

We now consider the term on the right hand side of this inequality.

$$\begin{aligned}
\|\hat{\mathbf{w}} - \mathbf{w}\|_p^p &= \sum_{j=1}^p |\hat{w}_j - w_j|^p \\
&= \sum_{j=1}^p \frac{|\hat{w}_j - w_j|^{p-1}}{\hat{w}_j + w_j} |\hat{w}_j^2 - w_j^2| \\
&= \sum_{j=1}^p \frac{|\hat{w}_j - w_j|^{p-1}}{\hat{w}_j + w_j} \sum_{k,l=1}^n q_n(\boldsymbol{\theta}^{(k)})q_n(\boldsymbol{\theta}^{(l)}) \left| \hat{k}_0^j(\boldsymbol{\theta}^{(k)}, \boldsymbol{\theta}^{(l)}) - k_0^j(\boldsymbol{\theta}^{(k)}, \boldsymbol{\theta}^{(l)}) \right|.
\end{aligned}$$

Let  $\epsilon(N) = \max_k \|\hat{\mathbf{u}}(\boldsymbol{\theta}^{(k)}) - \mathbf{u}(\boldsymbol{\theta}^{(k)})\|_\infty$ . The approximate error for the Stein kernel can be derived as follows.

$$\begin{aligned}
& \left| \hat{k}_0^j(\boldsymbol{\theta}^{(k)}, \boldsymbol{\theta}^{(l)}) - k_0^j(\boldsymbol{\theta}^{(k)}, \boldsymbol{\theta}^{(l)}) \right| \\
& \leq k(\boldsymbol{\theta}^{(k)}, \boldsymbol{\theta}^{(l)}) \left| \hat{u}_j(\boldsymbol{\theta}^{(k)}) \hat{u}_j(\boldsymbol{\theta}^{(l)}) - u_j(\boldsymbol{\theta}^{(k)}) u_j(\boldsymbol{\theta}^{(l)}) \right| \\
& + \left| \nabla_{\boldsymbol{\theta}_j^{(l)}} k(\boldsymbol{\theta}^{(k)}, \boldsymbol{\theta}^{(l)}) \right| \left| \hat{u}_j(\boldsymbol{\theta}^{(k)}) - u_j(\boldsymbol{\theta}^{(k)}) \right| \\
& + \left| \nabla_{\boldsymbol{\theta}_j^{(k)}} k(\boldsymbol{\theta}^{(l)}, \boldsymbol{\theta}^{(k)}) \right| \left| \hat{u}_j(\boldsymbol{\theta}^{(l)}) - u_j(\boldsymbol{\theta}^{(l)}) \right| \\
& \leq \left[ k(\boldsymbol{\theta}^{(k)}, \boldsymbol{\theta}^{(l)}) \left\{ |\hat{u}_j(\boldsymbol{\theta}^{(k)})| + |u_j(\boldsymbol{\theta}^{(l)})| \right\} + 2 \left| \nabla_{\boldsymbol{\theta}_j^{(l)}} k(\boldsymbol{\theta}^{(k)}, \boldsymbol{\theta}^{(l)}) \right| \right] \epsilon(N) \\
& \leq c_1 \epsilon(N)
\end{aligned} \tag{14}$$

for bounded constant  $c_1$ . The inequality in (14) follows from (9) and the fact that  $\nabla_{\boldsymbol{\theta}_j^{(l)}} k(\boldsymbol{\theta}^{(k)}, \boldsymbol{\theta}^{(l)})$  and  $\nabla_{\boldsymbol{\theta}_j^{(k)}} k(\boldsymbol{\theta}^{(l)}, \boldsymbol{\theta}^{(k)})$  are symmetric around zero. Now,

$$\begin{aligned}
\|\hat{\mathbf{w}} - \mathbf{w}\|_p^p & \leq c_1 \epsilon(N) \sum_{j=1}^p \frac{|\hat{w}_j - w_j|^{p-1}}{\hat{w}_j + w_j} \sum_{k,l=1}^n q_n(\boldsymbol{\theta}^{(k)}) q_n(\boldsymbol{\theta}^{(l)}) \\
& \leq n^2 c_1 c_2 \epsilon(N)
\end{aligned}$$

for bounded constant  $c_2$ . Therefore, the approximate error for AIKS is

$$\left| \hat{\mathcal{S}}(Q_n, \mathcal{T}_P, \mathcal{G}_{k, \|\cdot\|_p}) - \mathcal{S}(Q_n, \mathcal{T}_P, \mathcal{G}_{k, \|\cdot\|_p}) \right| \leq [n^2 M \epsilon(N)]^{1/p}$$

almost surely for bounded constant  $M$ .